

Analysis of anaerobic digestion model with two serial interconnected chemostats *

THAMER HMIDHI [†], RADHOUANE FEKIH-SALEM ^{*†‡}, and JÉRÔME HARMAND [§]

Abstract. In this paper, we study a well known two-step anaerobic digestion model in a configuration of two chemostats in series. This model is an eight-dimensional system of ordinary differential equations. Since the reaction system has a cascade structure, we show that the eight-order model can be reduced to a four-dimensional one. Using general growth rates, we provide an in-depth mathematical analysis of the asymptotic behavior of the system. First, we determine all the steady states of the model where there can be more than fifteen equilibria with a non-monotonic growth rate. Then, the necessary and sufficient conditions of existence and local stability of all steady states are established according to the operating parameters: the dilution rate, the input concentrations of the two nutrients, and the distribution of the total process volume considered. The operating diagrams are then analyzed theoretically to describe the asymptotic behavior of the process according to the four control parameters. There can be seventy regions with rich behavior where the system may exhibit bistability or tristability with the coexistence of both microbial species in the two bioreactors.

Key words. Anaerobic digestion, Bifurcation diagram, Coexistence, Interconnected chemostats, Stability.

MSC codes. 34A34, 34D20, 37N25, 92B05

1. Introduction. Anaerobic Digestion (AD) is a biological process in which organic matter is transformed by a complex microbial ecosystem into biogas in the absence of oxygen. It is used for the treatment of wastewater and the production of energy in the form of biogas containing methane. Under specific conditions, it may also be used to produce hydrogen from waste: the process is then named ‘black fermentation’. It is thus a fundamental process in the field of circular economy and green energy production from waste, [48].

On the one hand, biological are attractive: based on natural processes, they are relatively easy and simple to manage. On the other hand, they are usually considered as low yield and rate processes when compared to other energy producing processes. This why it is particularly important to optimize their design. In particular, in (bio)chemical engineering, one very important and actually quite old question is whether a biological process must be implemented in a homogeneous medium, or not. To study this question and characterize the mixing characteristics of the medium in a reactor, chemical engineers have proposed formal representations of chemical and biochemical devices known as ‘ideal’ (or ‘perfect’) reactors. On the one side of the scale on which reactors would be classified according to their homogeneity, there are the Completely Stirred Tank Reactors: they are completely mixed systems where the medium is considered as being perfectly homogeneous (CSTR). On the other side, we define the Plug Flow Reactors (PFR) which are nonhomogeneous systems in which small volumes of matter progress from the input to the output of the process independently of what happens around them. Practically, we can represent this situation with a long pipe of small diameter in which slices of little volumes of medium progress at a given speed without any exchange with those which go before and those which come after, the bioreaction taking place only inside each slice of liquid. Notice that a PFR may be approximated by an infinite number of CSTR in series. A limited number of CSTR is thus suited to represent situations between these two ideal cases, see for instance [31].

*Submitted to the editors 2024-08-05.

Funding: This work was supported by the Euro-Mediterranean research network TREASURE (<http://www.inra.fr/treasure>).

[†]University of Tunis El Manar, National Engineering School of Tunis, LAMSIN, Tunisia (thamer.hmidhi@enit.utm.tn).

[‡]University of Monastir, Higher Institute of Computer Science of Mahdia, Tunisia (radhouane.fekih-saleh@enit.utm.tn).

[§]LBE, University of Montpellier, INRAE, Narbonne, France (jerome.harmand@inrae.fr).

In microbiology/biotechnology, a CSTR is named ‘chemostat’. It consists in a tank filled with an aqueous solution in which microorganisms, generically named ‘biomass’, grow on one or more resources, named ‘substrates’. The first introduction of the chemostat dates back to 1950 by its inventors Novick and Szilard [38] simultaneously with Monod [32]. More than a common laboratory apparatus used for the continuous cultivation of microorganisms, its model has been studied as a mathematical object since its origins in the fifties [24, 46]. As such, it plays an important role as a model to study the growth of microbes and their interactions in mathematical biology and mathematical ecology. It has been long time used as a model of wastewater biological treatment processes and has been widely used to model industrial bioreactors.

Following the increasing knowledge accumulated over time about the anaerobic microbial ecosystems, the AD process is schematically represented as a set of bioreactions in cascade realized by several groups of microbes, the output of a reaction step being considered to be the input of the next one. Depending on the nature of its inputs, the AD is represented either as a one, two, three, or even four-step process, *cf.* for instance [51]. It is recognized that the most complete actual model is the ADM1 developed initially proposed by Batstone *et al.* [3, 29]. Of course, greater the complexity, lesser the possibility of analytically analyzing the properties of the associated model. Indeed, because of its complexity, and notably its relatively high dimension, the ADM1 is not easy to study from a mathematical viewpoint: very few studies were able to investigate its properties. From the best of our knowledge, there exists only one paper studying its steady states and their stability (see [7]). The AM2 model proposed by [6] is a two-step AD model. It is particularly interesting because it is of medium complexity. It has been shown to be able to represent real data in capturing the main dynamical features of different full-scale AD processes and is thus well suited for control design. During the last decade, many papers in the literature have studied the AM2 model and some of its extensions (see [4, 5, 19, 41]).

The ‘optimal design’ of a biological system consists in finding the ‘best configuration’ - in the sense of a given performance criterion - of this system. In particular, a major question in process engineering is to determine which type of reactor or interconnection of reactors - typically perfect reactors - is the most suitable to maximize such a performance for a given biological process, [21]. By ‘type or reactor’ or ‘interconnection of reactors’, we essentially mean determining whether it is important to favor a homogeneous medium (and thus use a chemostat), or not (and thus rather use an interconnection of chemostats, or even a PFR). Notice that there exist many alternative configurations, such as several chemostats working in parallel with or without convective or diffusive connections. Several mathematical studies have addressed these issues in considering what is named the ‘minimal chemostat model’, that is a single-step biological reaction and different biomass growth rates, see [9, 10, 11, 12, 22, 26, 27] for configurations involving chemostats in series, and [22, 31] for configurations of chemostats in parallel. For instance, considering the maximization of conversion yield, Haidar *et al.* [22] have shown that there exists a threshold on the concentration of nutrient supply for which the series and parallel configurations are better than a single chemostat at steady state. In [10], authors have compared the performances between the two serial interconnected chemostats and of a single chemostat and showed the most effective serial configuration of two chemostats against one to maximize the conversion of the substrate. Notice that if the objective is to maximize the productivity of biomass or, equivalently the production of biogas, the results may be different. And indeed, in the most general case, the results highly depend on both the growth rate considered, the input substrate concentration, and on the objective pursued. The papers cited hereabove are very general studies that did not consider specifically the AD process and only concentrated on the optimal design of single-step biological reactional systems. What about the optimal design of multiple-step processes as it is the case for the AD? In particular, do the results establish for a one-step system hold for a two-step process? In addition, one may further question whether a configuration in which only the first reaction would take place in one reactor (in which case the first reactor may be used to produce hydrogen) and the second reaction in another one

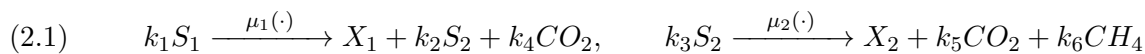
would be better than any other configuration of reactors, or not. Several authors have begun to address these questions either experimentally (*cf.* for instance [45]) or theoretically in using the minimal chemostat model in each stage (*cf.* for instance [8, 18, 39]). However, before addressing the problem of optimally designing multi-step biological processes, it is essential to study the properties of such a process in a cascade of chemostats, that are the existence and the steady states properties of the steady states.

In this work, we propose an original model describing the two-stage AD process in two series-connected chemostats. Using the same removal rates of two species in the two bioreactors, the eight-dimensional system with a cascade structure can be reduced to a four-dimensional system. Using monotonic growth rates for the first species and non-monotonic growth rates for the second species, we investigate the existence and stability of all steady states according to the control parameters. Moreover, we theoretically describe the operating diagrams and show that the model exhibits a very rich behavior, where there can be bistability and tristability with the coexistence of two populations of micro-organisms in each bioreactor.

Indeed, the operating diagram is a very useful tool for engineers, enabling them to graphically synthesize the asymptotic behavior of the process as a function of the control parameters. It was established in the book [24] for the classical chemostat model with Monod and Haldane growth rates. Three methods of analysis and construction of the operating diagram in the existing literature have been reported and summarized in Mtar et al [34]: purely numerical point-by-point [49, 50], by the numerical continuation of bifurcations through software packages such as MatCont (see [17] and the reference therein) and theoretical from the existence and stability conditions. We can cite the following papers based on the numerical study of the operating diagram as in [23, 30, 44, 50, 52, 53]. Several other recent papers have been based on the theoretical study of the operating diagram with various biological and ecological applications: anaerobic digestion [13, 19, 40, 41, 42, 51], microbial food webs [35, 36, 37, 43, 47] serially interconnected chemostats [9, 10, 11, 12], competition with inhibition and allelopathy effects [2, 14, 15, 16, 54] and density-dependence models [20, 33, 34].

This paper is organized as follows: in section 2, we propose a original model describing the AD process with a serial configuration of two chemostats. In section 3, we show that the study of the eight-dimension system can be reduced to a four-dimension one. Subsection 3.1 is devoted to analyzing the existence conditions and multiplicity of all steady states of the reduced model. Subsection 3.2 is dedicated to establishing the local stability conditions of all steady states. Then, in section 4, we establish theoretically the operating diagram from the existence and stability conditions. In section 5, we discuss our results by comparing them with those of the existing literature. The proofs of all results are reported in Appendix A. The parameter values used in all figures and the tables defining the various regions of the operating diagram are provided in Appendix B.

2. Modeling the configuration of two interconnected chemostats. We first recall the general two-step model in a single chemostat with a cascade of the following two biological reactions (see [6]):



where the organic substrate S_1 is consumed by acidogenic bacteria X_1 to produce a product S_2 (Volatile Fatty Acid). In the second reaction, the methanogenic bacteria X_2 consumes the substrate S_2 and produces biogas. μ_1 and μ_2 are the kinetics of the two reactions, k_i , $i = 1, \dots, 6$ are the pseudo-stoichiometric coefficients. The substrates S_1 and S_2 are introduced in the reactor with the inflowing concentrations S_1^{in} and S_2^{in} , respectively, with the input flow rate Q so that the dilution rate $D = Q/V$. Thus, we obtain the so-called AM2 model which is described by

the following ordinary differential equations:

$$(2.2) \quad \begin{cases} \dot{S}_1 &= D(S_1^{in} - S_1) - k_1\mu_1(\cdot)X_1, \\ \dot{X}_1 &= (\mu_1(\cdot) - \alpha D)X_1, \\ \dot{S}_2 &= D(S_2^{in} - S_2) + k_2\mu_1(\cdot)X_1 - k_3\mu_2(\cdot)X_2, \\ \dot{X}_2 &= (\mu_2(\cdot) - \alpha D)X_2, \end{cases}$$

where only a fraction α of the biomass is in the liquid phase. More precisely, $\alpha \in [0, 1]$ is a parameter allowing us to decouple the Hydraulic Retention Time (HRT) and the Solid Retention Time (SRT) (see [6] for more detail on the model development).

The AM2 model (2.2) has been studied in [5, 41, 44] when the growth rate μ_i for $i = 1, 2$ depends only on substrate S_i ($\mu_i(\cdot) = \mu_i(S_i)$), that is, (2.2) has a cascade-connected subsystems describing a commensalistic relationship. In [19], an in-depth mathematical study of model (2.2) has been established by considering a syntrophic relationship between the species, that is, $\mu_1(\cdot)$ depends on both substrates S_1 and S_2 while $\mu_2(\cdot)$ depends on the substrate S_2 ($\mu_1(\cdot) = \mu_1(S_1, S_2)$, $\mu_2(\cdot) = \mu_2(S_2)$). A summary review of the AM2 model for commensalistic and syntrophic relationships describing the modeling assumptions and the growth rates is provided in [19]. Recently, the maximization of biogas production of the AM2 model (2.2) was established theoretically according to the bioreactor control parameters [40].

In this paper, we consider a serial configuration of two interconnected chemostats where the volume V is divided into two volumes, $r_1V = rV$ and $r_2V = (1 - r)V$ with $r \in (0, 1)$ (see Figure 1). The two-tiered model we consider here describes the same biological reactions (2.1). However, the concentrations of substrate S_1 and S_2 and biomass X_1 and X_2 are different in each bioreactor, which we'll note as S_i^j and X_i^j , $i, j = 1, 2$ in each bioreactor j . Moreover, S_1^{in} and S_2^{in} are the concentrations of input substrate S_1^1 and S_2^1 in the first chemostat at a flow rate Q . The substrates S_1^2 and S_2^2 are introduced in the second chemostat with the inflowing concentrations S_1^1 and S_2^1 , respectively, and a flow rate Q .

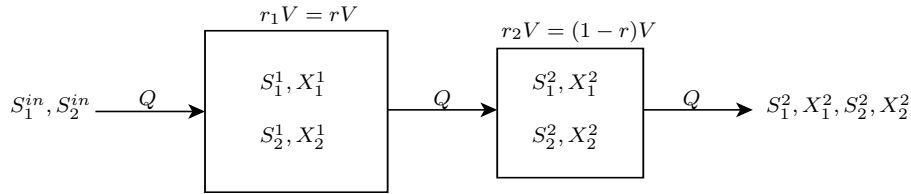


Figure 1. The serial configuration of two interconnected chemostats.

Using Antoine Lavoisier's law: "Nothing is lost, nothing is created, everything is transformed" and establishing the mass balance between the instants t and $t + dt$, we obtain the mathematical model given by the following eight-dimensional system of ordinary differential equations:

$$(2.3) \quad \begin{cases} \dot{S}_1^1 &= D_1(S_1^{in} - S_1^1) - k_1\mu_1(S_1^1)X_1^1, \\ \dot{X}_1^1 &= (\mu_1(S_1^1) - D_1)X_1^1, \\ \dot{S}_2^1 &= D_1(S_2^{in} - S_2^1) + k_2\mu_1(S_1^1)X_1^1 - k_3\mu_2(S_2^1)X_2^1, \\ \dot{X}_2^1 &= (\mu_2(S_2^1) - D_1)X_2^1, \\ \dot{S}_1^2 &= D_2(S_1^1 - S_1^2) - k_1\mu_1(S_1^2)X_1^2, \\ \dot{X}_1^2 &= D_2(X_1^1 - X_1^2) + \mu_1(S_1^2)X_1^2, \\ \dot{S}_2^2 &= D_2(S_2^1 - S_2^2) + k_2\mu_1(S_1^2)X_1^2 - k_3\mu_2(S_2^2)X_2^2, \\ \dot{X}_2^2 &= D_2(X_2^1 - X_2^2) + \mu_2(S_2^2)X_2^2, \end{cases}$$

where $D_1 = D/r_1$ and $D_2 = D/r_2$ are the dilution rates corresponding to the first and second chemostats, respectively. In this paper, we assume that the growth functions $\mu_1(S_1)$ and $\mu_2(S_2)$ belongs to $\mathcal{C}^1(R_+)$ and satisfy the following hypotheses.

Hypothesis 2.1. $\mu_1(0) = 0$, $\mu_1(+\infty) = m_1$, and $\mu'_1(S_1) > 0$ for all $S_1 > 0$.

Hypothesis 2.2. $\mu_2(0) = 0$, $\mu_2(+\infty) = 0$, and there exists $S_2^m > 0$ such that $\mu'_2(S_2) > 0$, for all $0 < S_2 < S_2^m$ and $\mu'_2(S_2) < 0$, for all $S_2 > S_2^m$.

Hypothesis 2.1 means that the substrate is necessary for the growth of the first species. In addition, the growth rate of the first species is favored by the concentration of the substrate S_1 . *Hypothesis 2.2* means that the growth of the second species takes into account the growth-limiting for low concentrations of substrate S_2 and the growth-inhibiting for high concentrations.

To preserve the biological meaning of our model (2.3), we prove the following result. Since the proof is classical, it is left to the reader.

Proposition 2.3. *All solutions of model (2.3) with nonnegative initial condition remain non-negative and bounded for all positive times. Let $\xi = (S_1^1, X_1^1, S_2^1, X_2^1, S_1^2, X_1^2, S_2^2, X_2^2)$ be the state vector. The set*

$$\Omega = \{\xi \in \mathbb{R}_+^8 : S_1^i + k_1 X_1^i = S_1^{in} \text{ and } S_2^i + k_3 X_2^i - k_2 X_1^i = S_2^{in}, i = 1, 2\}$$

is positively invariant and is a global attractor for (2.3).

3. Reduced model. In the following, we show that the existence and asymptotic stability of the steady states of the eight-dimensional system (2.3) can be deduced from that of the four-dimensional system (3.2). The change of variable

$$Z_1^i = S_1^i + k_1 X_1^i \quad \text{and} \quad Z_2^i = S_2^i + k_3 X_2^i - k_2 X_1^i, \quad i = 1, 2,$$

transforms system (2.3) into a system having the same structure, namely a system of the form

$$(3.1) \quad \begin{cases} \dot{Z}_1^1 &= D_1 (S_1^{in} - Z_1^1), \\ \dot{Z}_2^1 &= D_1 (S_2^{in} - Z_2^1), \\ \dot{Z}_1^2 &= D_2 (Z_1^1 - Z_1^2), \\ \dot{Z}_2^2 &= D_2 (Z_2^1 - Z_2^2), \\ \dot{X}_1^1 &= (\mu_1 (Z_1^1 - k_1 X_1^1) - D_1) X_1^1, \\ \dot{X}_2^1 &= (\mu_2 (Z_2^1 + k_2 X_1^1 - k_3 X_2^1) - D_1) X_2^1, \\ \dot{X}_1^2 &= D_2 (X_1^1 - X_1^2) + \mu_1 (Z_1^2 - k_1 X_1^2) X_1^2, \\ \dot{X}_2^2 &= D_2 (X_2^1 - X_2^2) + \mu_2 (Z_2^2 + k_2 X_1^2 - k_3 X_2^2) X_2^2. \end{cases}$$

Thus, the steady states of the eight-dimension system (2.3) are given by the steady state of (3.1). From the first four equations of (3.1), we see that a steady state of (3.1) must satisfy $Z_i^j = S_i^{in}$, $i, j = 1, 2$. Setting $Z_i^j = S_i^{in}$ in the lower subsystem of (3.1), we obtain the following reduced system

$$(3.2) \quad \begin{cases} \dot{X}_1^1 &= (\mu_1 (S_1^{in} - k_1 X_1^1) - D_1) X_1^1, \\ \dot{X}_2^1 &= (\mu_2 (S_2^{in} + k_2 X_1^1 - k_3 X_2^1) - D_1) X_2^1, \\ \dot{X}_1^2 &= D_2 (X_1^1 - X_1^2) + \mu_1 (S_1^{in} - k_1 X_1^2) X_1^2, \\ \dot{X}_2^2 &= D_2 (X_2^1 - X_2^2) + \mu_2 (S_2^{in} + k_2 X_1^2 - k_3 X_2^2) X_2^2. \end{cases}$$

Hence, the last four components of a steady state of the eight-dimensional system (3.1) are given by putting the left-hand side of the reduced system (3.2) equal to zero. Thus, for each steady state of the four-dimensional system (3.2) denoted by

$$\mathcal{E}_{ij}^{kl} (X_1^1, X_2^1, X_1^2, X_2^2), \quad \{i, j, k, l\} \in \{0, 1, 2\}$$

corresponds a steady state of the eight-dimensional system (2.3) denoted by

$$\mathcal{F}_{ij}^{kl} (S_1^1, X_1^1, S_2^1, X_2^1, S_1^2, X_1^2, S_2^2, X_2^2)$$

where

$$S_1^i = S_1^{in} - k_1 X_1^i \quad \text{and} \quad S_2^i = S_2^{in} - k_3 X_2^i + k_2 X_1^i, i = 1, 2.$$

To analyze the local stability of each steady state, system (3.1) possesses a pair of cascade-connected subsystems in the (ξ_1, ξ_2) coordinates of the form (see e.g. [28])

$$\begin{cases} \dot{\xi}_1 = f(\xi_1) \\ \dot{\xi}_2 = g(\xi_2, \xi_1), \end{cases}$$

where

$$f(\xi_1) = \begin{bmatrix} D_1 (S_1^{in} - Z_1^1) \\ D_1 (S_2^{in} - Z_2^1) \\ D_2 (Z_1^1 - Z_1^2) \\ D_2 (Z_2^1 - Z_2^2) \end{bmatrix}, \quad g(\xi_2, \xi_1) = \begin{bmatrix} (\mu_1 (Z_1^1 - k_1 X_1^1) - D_1) X_1^1 \\ (\mu_2 (Z_2^1 + k_2 X_1^1 - k_3 X_2^1) - D_1) X_2^1 \\ D_2 (X_1^1 - X_1^2) + \mu_1 (Z_1^2 - k_1 X_1^2) X_1^2, \\ D_2 (X_2^1 - X_2^2) + \mu_2 (Z_2^2 + k_2 X_1^2 - k_3 X_2^2) X_2^2 \end{bmatrix}$$

where $\xi_1 = (Z_1^1, Z_2^1, Z_1^2, Z_2^2) \in \mathbb{R}_+^4$ and $\xi_2 = (X_1^1, X_2^1, X_1^2, X_2^2) \in \mathbb{R}_+^4$. So that

$$g(\xi_1^*) = 0, \quad g(\xi_2^*, \xi_1^*) = 0,$$

Note that ξ_1^* is LES of the upper subsystem of (3.1) since at ξ_1^* , the characteristic polynomial is

$$P(\lambda) = (D_1 + \lambda)^2 (D_2 + \lambda)^2.$$

Using [28, Corollary 10.3.2], we show that the local stability of ξ_2^* of the lower subsystem $\dot{\xi}_2 = g(\xi_2, \xi_1^*)$ is the same as the one of the cascade (3.1) at $(\xi_1, \xi_2) = (\xi_1^*, \xi_2^*)$.

Since the components S_1^1, S_2^1, S_1^2 and S_2^2 are nonnegative, system (3.2) is defined on the set:

$$(3.3) \quad M = \left\{ (X_1^1, X_2^1, X_1^2, X_2^2) \in \mathbb{R}_+^4 : X_1^i \leq \frac{S_1^{in}}{k_1} \text{ and } X_2^i \leq \frac{S_2^{in} + k_2 X_1^i}{k_3}, i = 1, 2 \right\}.$$

3.1. Existence and multiplicity of the steady states. A steady state exists if and only if all its components are nonnegative. Each steady state is preceded by a subscript and an exponent, indicating which population of microorganisms survives in the first and the second chemostat, respectively. For example, the subscript in \mathcal{E}_{0i}^{11} , $i = 1, 2$ implies that $X_1^1 = 0$ and $X_2^1 > 0$ with the possibility of two different concentrations of X_2^1 at the steady state. However, the exponent in \mathcal{E}_{0i}^{11} implies that $X_1^2 > 0$ and $X_2^2 > 0$. Indeed, system (3.2) has the following nine types of steady states with $i = 1, 2$.

- $\mathcal{E}_{00}^{00} (X_1^1 = 0, X_2^1 = 0, X_1^2 = 0, X_2^2 = 0)$: washout of the two species in each bioreactor.
- $\mathcal{E}_{00}^{0i} (X_1^1 = 0, X_2^1 = 0, X_1^2 = 0, X_2^2 > 0)$: only the second species is in the second bioreactor.
- $\mathcal{E}_{00}^{10} (X_1^1 = 0, X_2^1 = 0, X_1^2 > 0, X_2^2 = 0)$: only the first species is in the second bioreactor.
- $\mathcal{E}_{00}^{1i} (X_1^1 = 0, X_2^1 = 0, X_1^2 > 0, X_2^2 > 0)$: only the two species is in the second bioreactor.
- $\mathcal{E}_{10}^{10} (X_1^1 > 0, X_2^1 = 0, X_1^2 > 0, X_2^2 = 0)$: only the first species is in each bioreactor.
- $\mathcal{E}_{10}^{1i} (X_1^1 > 0, X_2^1 = 0, X_1^2 > 0, X_2^2 > 0)$: exclusion of the second species in the first bioreactor.
- $\mathcal{E}_{0i}^{01} (X_1^1 = 0, X_2^1 > 0, X_1^2 = 0, X_2^2 > 0)$: only the second species is in each bioreactor.
- $\mathcal{E}_{0i}^{11} (X_1^1 = 0, X_2^1 > 0, X_1^2 > 0, X_2^2 > 0)$: exclusion of the first species in the first bioreactor.
- $\mathcal{E}_{1i}^{11} (X_1^1 > 0, X_2^1 > 0, X_1^2 > 0, X_2^2 > 0)$: the two species in each bioreactor are maintained.

To describe the steady states of (3.2), we define in Table 1 the following auxiliary functions depending on the operating parameters D, r, S_1^{in} , and S_2^{in} . To simplify the notations, we will denote in the following

$$\lambda_1^i = \lambda_1^i(D, r) \quad \text{and} \quad \lambda_2^{ij} = \lambda_2^{ij}(D, r), \quad i, j = 1, 2.$$

On the other hand, to establish the existence and multiplicity of steady states of (3.2), we also need to define some auxiliary functions listed in Table 2. In the following proposition, we provide the necessary and sufficient conditions for the existence of all steady states of model (3.2).

Table 1

Auxiliary functions depending on D , r , S_1^{in} , and S_2^{in} for $i, j = 1, 2$ where $D_i := D/r_i$, $D_i^m := r_i \mu_2(S_2^m)$, $r_1 = r$, $r_2 = 1 - r$, and X_1^{2*} is the unique solution of equation $f_1(x) = g_1(x)$ with the functions f_1 and g_1 are defined in Table 2.

	Definition
$\lambda_1^i(D, r)$	$\lambda_1^i(D, r)$ is the unique solution of equation $\mu_1(S_1) = D_i$. It is defined for $0 < D < r_i m_1$. If $D \geq r_i m_1$, by convention we let $\lambda_1^i(D, r) = +\infty$.
$\lambda_2^{ij}(D, r)$	$\lambda_2^{i1}(D, r) < \lambda_2^{i2}(D, r)$ are the two solutions of equation $\mu_2(S_2) = D_i$. They are defined for $0 < D \leq D_i^m$. If $D > D_i^m$, by convention we let $\lambda_2^{ij}(D, r) = +\infty$.
$F_{1j}(D, r, S_2^{in})$	$F_{1j}(D, r, S_2^{in}) = \lambda_1^1(D, r) + \frac{k_1}{k_2} (\lambda_2^{1j}(D, r) - S_2^{in})$. It is defined for $0 < D < \min(r_1 m_1, D_1^m)$.
$F_{2j}(D, r, S_2^{in})$	$F_{2j}(D, r, S_2^{in}) = \lambda_1^2(D, r) + \frac{k_1}{k_2} (\lambda_2^{2j}(D, r) - S_2^{in})$. It is defined for $0 < D < \min(r_2 m_1, D_2^m)$.
$\phi_j(D, r, S_1^{in}, S_2^{in})$	$\phi_j(D, r, S_1^{in}, S_2^{in}) = S_2^{in} + k_2 X_1^{2*}(D, r, S_1^{in}) - \lambda_2^{2j}(D, r)$. It is defined for $0 < D \leq D_2^m$ and $S_1^{in} > \lambda_1^1$.

Table 2

Auxiliary functions and their domains of definition. Note that X_1^{1*} , X_2^{1*} , X_1^{2*} are the components of different steady state in Table 3, and $k_i, i = 1, 2, 3$ are the pseudo-stoichiometric coefficients.

Auxiliary functions	Domains of definition
$g_1(x) := D_2 \left(\frac{x - X_1^{1*}}{x} \right)$	$x \in (0, +\infty)$
$g_2(x) := D_2 \left(\frac{x - X_2^{1*}}{x} \right)$	$x \in (0, +\infty)$
$f_1(x) := \mu_1(S_1^{in} - k_1 x)$	$x \in [0, S_1^{in}/k_1]$
$f_2(x) := \mu_2(S_2^{in} - k_3 x)$	$x \in [0, S_2^{in}/k_3]$
$f_3(x) := \mu_2(S_2^{in} + k_2 X_1^{2*} - k_3 x)$	$x \in [0, (S_2^{in} + k_2 X_1^{2*})/k_3]$

Proposition 3.1. Assume that *Hypotheses 2.1* and *2.2* hold. Then, the nine types of steady states of (3.2) are given in Table 3. Their existence conditions are given in Table 4.

The following proposition determines the existence and multiplicity of steady states of (3.2).

Proposition 3.2. Assume that *Hypotheses 2.1* and *2.2*, and the existence conditions in Table 4 hold for the steady states \mathcal{E}_{00}^{kl} , \mathcal{E}_{10}^{1l} , \mathcal{E}_{0i}^{k1} and \mathcal{E}_{1i}^{11} , $i = 1, 2$, $k = 0, 1$, and $l = 0, 1, 2$.

- The steady states \mathcal{E}_{00}^{kl} , \mathcal{E}_{10}^{1l} and \mathcal{E}_{01}^{01} are unique.
- There exists at least one steady state of the form \mathcal{E}_{02}^{01} . Generically, the system has an odd number of steady states of the form \mathcal{E}_{02}^{01} .
- If $X_2^{1*} > x_2^m$, the steady state \mathcal{E}_{0i}^{11} and \mathcal{E}_{1i}^{11} are unique. If $X_2^{1*} < x_2^m$, then there exists at least one steady state of the form \mathcal{E}_{0i}^{11} and \mathcal{E}_{1i}^{11} . Generically, the system has an odd number of steady states of the form \mathcal{E}_{0i}^{11} and \mathcal{E}_{1i}^{11} , $i = 1, 2$.

3.2. Local stability of steady states. The following result provides the local stability condition of each steady state of system (3.2). For convenience, we shall use the abbreviation LES for Locally Exponentially Stable.

Proposition 3.3. Assume that *Hypotheses 2.1* and *2.2* hold. The steady states \mathcal{E}_{00}^{02} , \mathcal{E}_{00}^{12} , \mathcal{E}_{10}^{12} , \mathcal{E}_{02}^{01} , \mathcal{E}_{02}^{11} and \mathcal{E}_{12}^{11} of system (3.2) are unstable when they exist. The conditions stability of all other steady states are given in Table 5.

4. Operating diagrams. In this section, we study theoretically the operating diagrams that describe the asymptotic behavior of the process according to four control parameters D , S_1^{in} , S_2^{in} ,

Table 3

Components of all steady states of (3.2). The functions $\lambda_1^i, \lambda_2^i, \lambda_2^{2i}, F_{ij}$ and $\phi_i, i, j = 1, 2$ are defined in Table 1 while the functions f_1, f_2, f_3, g_1 and g_2 are defined in Table 2.

(X_1^{1*}, X_2^{1*})	(X_1^{2*}, X_2^{2*})
$\mathcal{E}_{00}^{00} (0, 0)$	$(0, 0)$
$\mathcal{E}_{00}^{0i} (0, 0)$	$(0, (S_2^{in} - \lambda_2^{2i}) / k_3)$
$\mathcal{E}_{00}^{10} (0, 0)$	$(\frac{1}{k_1} (S_1^{in} - \lambda_1^2), 0)$
$\mathcal{E}_{00}^{1i} (0, 0)$	$((S_1^{in} - \lambda_1^2) / k_1, k_2 (S_1^{in} - F_{2i}) / (k_1 k_3))$
$\mathcal{E}_{10}^{10} ((S_1^{in} - \lambda_1^1) / k_1, 0)$	$(X_1^{2*}, 0)$ X_1^{2*} is the unique solution of $f_1(x) = g_1(x)$
$\mathcal{E}_{10}^{1i} ((S_1^{in} - \lambda_1^1) / k_1, 0)$	$(X_1^{2*}, \phi_i / k_3)$ X_1^{2*} is the unique solution of $f_1(x) = g_1(x)$
$\mathcal{E}_{0i}^{01} (0, (S_2^{in} - \lambda_2^{1i}) / k_3)$	$(0, X_2^{2*})$ X_2^{2*} is a solution of $f_2(X_2^2) = g_2(X_2^2)$
$\mathcal{E}_{0i}^{11} (0, (S_2^{in} - \lambda_2^{1i}) / k_3)$	$((S_1^{in} - \lambda_1^2) / k_1, X_2^{2*})$ X_2^{2*} is a solution of $f_3(x) = g_2(x)$
$\mathcal{E}_{1i}^{11} (\frac{1}{k_1} (S_1^{in} - \lambda_1^1), \frac{k_2}{k_1 k_3} (S_1^{in} - F_{1i}))$	X_1^{2*} is a unique solution of $f_1(x) = g_1(x)$ X_2^{2*} is a solution of $f_3(x) = g_2(x)$

Table 4

Existence condition of steady states of system (3.2) where X_1^{2*} is a unique solution of equation $f_1(x) = g_1(x)$. The functions $\lambda_1^i, \lambda_2^i, \lambda_2^{2i}, F_{ij}$ and $\phi_i, i, j = 1, 2$ are defined in Table 1 and the functions f_1 and g_1 are defined in Table 2.

	Existence conditions
\mathcal{E}_{00}^{00}	Always exists
\mathcal{E}_{00}^{0i}	$S_2^{in} > \lambda_2^{2i}$
\mathcal{E}_{00}^{10}	$S_1^{in} > \lambda_1^2$
\mathcal{E}_{00}^{1i}	$S_1^{in} > \max(\lambda_1^2, F_{2i})$
\mathcal{E}_{10}^{10}	$S_1^{in} > \lambda_1^1$
\mathcal{E}_{10}^{1i}	$S_1^{in} > \lambda_1^1$ and $\phi_i > 0$
\mathcal{E}_{0i}^{01}	$S_2^{in} > \lambda_2^{1i}$
\mathcal{E}_{0i}^{11}	$S_1^{in} > \lambda_1^2$ and $S_2^{in} > \lambda_2^{1i}$
\mathcal{E}_{1i}^{11}	$S_1^{in} > \max(\lambda_1^1, F_{1i})$

Table 5

The stability condition of steady states of system (3.2) except for $\mathcal{E}_{00}^{02}, \mathcal{E}_{00}^{12}, \mathcal{E}_{10}^{12}, \mathcal{E}_{02}^{01}, \mathcal{E}_{02}^{11}$ and \mathcal{E}_{12}^{11} which are unstable. The functions f_1, f_3, g_1 and g_2 are defined in Table 2 while X_1^{2*} is a unique solution of equation $f_1(x) = g_1(x)$ and X_2^{2*} is a solution of $f_3(x) = g_2(x)$.

	Stability conditions
\mathcal{E}_{00}^{00}	$S_1^{in} < \min(\lambda_1^1, \lambda_1^2)$ and $S_2^{in} \notin [\min(\lambda_2^{11}, \lambda_2^{21}), \max(\lambda_2^{12}, \lambda_2^{22})]$
\mathcal{E}_{00}^{01}	$S_1^{in} < \min(\lambda_1^1, \lambda_1^2)$ and $S_2^{in} \notin [\lambda_2^{11}, \lambda_2^{12}]$
\mathcal{E}_{00}^{10}	$S_1^{in} < \lambda_1^1, S_2^{in} \notin [\lambda_2^{11}, \lambda_2^{12}]$ and $S_2^{in} + \frac{k_2}{k_1} (S_1^{in} - \lambda_1^2) \notin [\lambda_2^{21}, \lambda_2^{22}]$
\mathcal{E}_{00}^{11}	$S_1^{in} < \lambda_1^1$ and $S_2^{in} \notin [\lambda_2^{11}, \lambda_2^{12}]$
\mathcal{E}_{10}^{10}	$S_2^{in} + \frac{k_2}{k_1} (S_1^{in} - \lambda_1^1) \notin [\lambda_2^{11}, \lambda_2^{12}]$ and $\phi_1 < 0$ or $\phi_2 > 0$
\mathcal{E}_{10}^{11}	$S_2^{in} + \frac{k_2}{k_1} (S_1^{in} - \lambda_1^1) \notin [\lambda_2^{11}, \lambda_2^{12}]$
\mathcal{E}_{01}^{01}	$S_1^{in} < \min(\lambda_1^1, \lambda_1^2)$
\mathcal{E}_{01}^{11}	$S_1^{in} < \lambda_1^1$ and $g_2'(X_2^{2*}) > f_3'(X_2^{2*})$
\mathcal{E}_{11}^{11}	$g_2'(X_2^{2*}) > f_3'(X_2^{2*})$

and r which are the easiest parameters to manipulate in a chemostat. It is the best tool presented for the biologist to understand the asymptotic behavior of the process according to the operating parameters. However, since it is difficult to visualize all the regions of the operating diagrams in the four-dimensional space, we fix two parameters and release two others to illustrate these diagrams in the plan. In [subsection 4.1](#), it is analyzed in the two-dimensional plane (D, S_1^{in}) by fixing the parameter S_2^{in} and r . In [subsection 4.2](#), we fix D and r , and we determine the operating diagrams in the plane (S_2^{in}, S_1^{in}) . The other cases can be treated similarly. To determine the different regions in the operating diagram, we must define the surfaces γ_i , $i = 1, \dots, 15$, listed in [Table 6](#). They are obtained from the existence and stability conditions given in [Tables 4](#) and [5](#). They correspond to the boundaries of the change in the number of steady states in the positive octant and/or their local asymptotic behavior.

Table 6

Definitions of the surfaces γ_i , $i = 1, \dots, 15$. The functions F_{ij} and ϕ_j , $i, j = 1, 2$ are defined in [Table 1](#) and X_1^{2*} is the unique solution of equation $f_1(x) = g_1(x)$.

Curve γ_i
$\gamma_0 = \{(D, S_1^{in}, S_2^{in}, r) : S_1^{in} = \lambda_1^1(D, r), D \in [0, r_1 m_1)\}$
$\gamma_1 = \{(D, S_1^{in}, S_2^{in}, r) : S_1^{in} = \lambda_1^2(D, r), D \in [0, r_2 m_1)\}$
$\gamma_2 = \{(D, S_1^{in}, S_2^{in}, r) : S_1^{in} = F_{21}(D, r, S_2^{in}), D \in (0, r_2 \min(m_1, \mu_2(S_2^m)))\}$
$\gamma_3 = \{(D, S_1^{in}, S_2^{in}, r) : S_1^{in} = F_{22}(D, r, S_2^{in}), D \in (0, r_2 \min(m_1, \mu_2(S_2^m)))\}$
$\gamma_4 = \{(D, S_1^{in}, S_2^{in}, r) : S_1^{in} = F_{11}(D, r, S_2^{in}), D \in (0, r_1 \min(m_1, \mu_2(S_2^m)))\}$
$\gamma_5 = \{(D, S_1^{in}, S_2^{in}, r) : S_1^{in} = F_{12}(D, r, S_2^{in}), D \in (0, r_1 \min(m_1, \mu_2(S_2^m)))\}$
$\gamma_6 = \{(D, S_1^{in}, S_2^{in}, r) : D = D_1^* := r_1 \mu_2(S_2^{in})\}$
$\gamma_7 = \{(D, S_1^{in}, S_2^{in}, r) : D = D_2^* := r_2 \mu_2(S_2^{in})\}$
$\gamma_8 = \{(D, S_1^{in}, S_2^{in}, r) : D = D_1^m := r_1 \mu_2(S_2^m)\}$
$\gamma_9 = \{(D, S_1^{in}, S_2^{in}, r) : D = D_2^m := r_2 \mu_2(S_2^m)\}$
$\gamma_{10} = \{(D, S_1^{in}, S_2^{in}, r) : S_2^{in} = S_{21}^{in*} = \lambda_2^{11}(D, r), D < D_1^m\}$
$\gamma_{11} = \{(D, S_1^{in}, S_2^{in}, r) : S_2^{in} = S_{22}^{in*} = \lambda_2^{21}(D, r), D < D_2^m\}$
$\gamma_{12} = \{(D, S_1^{in}, S_2^{in}, r) : S_2^{in} = S_{23}^{in*} = \lambda_2^{12}(D, r), D < D_1^m\}$
$\gamma_{13} = \{(D, S_1^{in}, S_2^{in}, r) : S_2^{in} = S_{24}^{in*} = \lambda_2^{22}(D, r), D < D_2^m\}$
$\gamma_{14} = \{(D, S_1^{in}, S_2^{in}, r) : \phi_1(D, r, S_1^{in}, S_2^{in}) = 0, D \leq D_2^m \text{ and } S_1^{in} > \lambda_1^1\}$
$\gamma_{15} = \{(D, S_1^{in}, S_2^{in}, r) : \phi_2(D, r, S_1^{in}, S_2^{in}) = 0, D \leq D_2^m \text{ and } S_1^{in} > \lambda_1^1\}$

- Remark 4.1.** 1. Note that for all $D < D_1^m$, (or equivalently $D < r_1 \mu_2(S_2^m)$), the equation $\mu_2(S_2^{in}) = D_1 := D/r_1$ is equivalent to $S_2^{in} = \lambda_2^{11}$ or $S_2^{in} = \lambda_2^{12}$. From [Table 6](#), we see that $\gamma_6 = \gamma_{10} \cup \gamma_{12}$. Similarly, for all $D < D_2^m$, (or equivalently $D < r_2 \mu_2(S_2^m)$), the equation $\mu_2(S_2^{in}) = D_2 := D/r_2$ is equivalent to $S_2^{in} = \lambda_2^{21}$ or $S_2^{in} = \lambda_2^{22}$. From [Table 6](#), we see that $\gamma_7 = \gamma_{11} \cup \gamma_{13}$.
2. Let r be fixed. When S_2^{in} is fixed, the curves γ_6 and γ_7 are vertical lines in the plan (D, S_1^{in}) with equation $D = D_1^* := r_1 \mu_2(S_2^{in})$ and $D = D_2^* := r_2 \mu_2(S_2^{in})$, respectively. When D is fixed, the curve γ_i , $i = 10, \dots, 13$ is a vertical line in the plan (S_2^{in}, S_1^{in}) with equation $S_2^{in} = S_{2j}^{in*}$, $j = 1, \dots, 4$.

Using the definitions of the break-even concentrations λ_1^i and λ_2^{ij} , $i, j = 1, 2$, the following proposition determines the relative positions of these critical values according to the distribution of the total volume $r \in (0, 1)$.

Lemma 4.2. Assume that [Hypotheses 2.1](#) and [2.2](#) hold.

- If $r \in (0, 1/2)$, then $\lambda_1^2(D, r) < \lambda_1^1(D, r)$, $\lambda_2^{21}(D, r) < \lambda_2^{11}(D, r) < \lambda_2^{12}(D, r) < \lambda_2^{22}(D, r)$.
- If $r \in (1/2, 1)$, then $\lambda_1^1(D, r) < \lambda_1^2(D, r)$, $\lambda_2^{11}(D, r) < \lambda_2^{21}(D, r) < \lambda_2^{22}(D, r) < \lambda_2^{12}(D, r)$.
- If $r = 1/2$, then $\lambda_1^1(D, r) = \lambda_1^2(D, r)$, $\lambda_2^{11}(D, r) = \lambda_2^{21}(D, r)$, $\lambda_2^{12}(D, r) = \lambda_2^{22}(D, r)$.

4.1. . Operating diagram in the plane (D, S_1^{in}) when S_2^{in} and r are fixed. Fix r and S_2^{in} . In

this case, the surfaces γ_i correspond to curves for $i = 0, \dots, 5$ and vertical lines for $i = 6, \dots, 9$. Depending on the critical values m_1 , $\mu_2(S_2^{in})$, and $\mu_2(S_2^m)$, the following three cases should be distinguished in the operating diagram study when $r \in (0, 1/2)$ or $r \in (1/2, 1)$:

$$(4.1) \quad \text{case 1: } m_1 > \mu_2(S_2^m), \quad \text{case 2: } \mu_2(S_2^{in}) > m_1, \quad \text{case 3: } \mu_2(S_2^m) > m_1 > \mu_2(S_2^{in}).$$

Note that for each case in (4.1), S_2^{in} may be less than or greater than S_2^m . In this section, we present cases 1 and 2 for $r \in (0, 1/2)$ and case 1 for $r \in (1/2, 1)$. However, the study is similar in the other cases.

From the definitions of the auxiliary functions in Table 1, the following proposition establishes the relative positions of surfaces γ_i , $i = 0, \dots, 5$ according to the critical values D_1^* and D_2^* defined in Table 6.

Proposition 4.3. *Let $r \in (0, 1)$. If $m_1 > \mu_2(S_2^{in})$, then the curve γ_0 and the vertical line γ_6 intersect at the point $P_1(S_2^{in}, r) = (D_1^*, \lambda_1^1(D_1^*, r))$ in the plane (D, S_1^{in}) (see Figure 2 and Figure 10(a)). If, in addition, $S_2^{in} \geq S_2^m$, then γ_0 , γ_5 , and γ_6 intersect at the same point P_1 . Otherwise, when $S_2^{in} < S_2^m$, then γ_0 , γ_4 , and γ_6 intersect at the same point P_1 . Moreover:*

- If $D < D_1^*$, then $F_{11}(D, r, S_2^{in}) < \lambda_1^1(D, r) < F_{12}(D, r, S_2^{in})$.
- If $D > D_1^*$ and $S_2^{in} \geq S_2^m$, then $F_{11}(D, r, S_2^{in}) < F_{12}(D, r, S_2^{in}) < \lambda_1^1(D, r)$.
- If $D > D_1^*$ and $S_2^{in} < S_2^m$, then $\lambda_1^1(D, r) < F_{11}(D, r, S_2^{in}) < F_{12}(D, r, S_2^{in})$.

If $m_1 > \mu_2(S_2^{in})$, the curve γ_1 and the vertical line γ_7 intersect at $P_2(S_2^{in}, r) = (D_2^*, \lambda_1^2(D_2^*, r))$ in the plane (D, S_1^{in}) (see Figure 2 and Figure 10(a)). If, in addition, $S_2^{in} \geq S_2^m$, then γ_1 , γ_3 , and γ_7 intersect at the same point P_2 . Otherwise, when $S_2^{in} < S_2^m$, then γ_1 , γ_2 , and γ_7 intersect at the same point P_2 . Moreover:

- If $D < D_2^*$, then $F_{21}(D, r, S_2^{in}) < \lambda_1^2(D, r) < F_{22}(D, r, S_2^{in})$.
- If $D > D_2^*$ and $S_2^{in} \geq S_2^m$, then $F_{21}(D, r, S_2^{in}) < F_{22}(D, r, S_2^{in}) < \lambda_1^2(D, r)$.
- If $D > D_2^*$ and $S_2^{in} < S_2^m$, then $\lambda_1^2(D, r) < F_{21}(D, r, S_2^{in}) < F_{22}(D, r, S_2^{in})$.

The asymptotic behavior of system (2.3) varies according to the value of r in the intervals $(0, 1/2)$ and $(1/2, 1)$ such that the position of the various curves changes with r . The following proposition establishes the relative positions of the curves γ_2 and γ_4 when $S_2^{in} > S_2^m$.

Proposition 4.4. *Let $S_2^{in} > S_2^m$.*

- If $r \in (0, 1/2)$, then $F_{21}(D, r, S_2^{in}) < F_{11}(D, r, S_2^{in})$.
- If $r \in (1/2, 1)$, then $F_{21}(D, r, S_2^{in}) > F_{11}(D, r, S_2^{in})$.

Now to construct the operating diagrams, the growth rates μ_1 and μ_2 are chosen of Monod and Haldane type which are written:

$$(4.2) \quad \mu_1(S_1) = \frac{m_1 S_1}{k_{S_1} + S_1} \quad \text{and} \quad \mu_2(S_2) = \frac{m_2 S_2}{k_{S_2} + S_2 + \frac{(S_2)^2}{k_I}},$$

where m_i is the maximum growth rate and k_{S_i} is the half-saturation (or Michaelis-Menten) constant associated to S_i , for $i = 1, 2$. However, the construction can be applied to any growth rate verifying Hypotheses 2.1 and 2.2. The biological parameter values used in all figures are provided in Table 12. Note that we have used the same specific growth rates of Monod and Haldane types (4.2) and parameter values as in [6], with the exception of the maximum growth rate m_1 to have a richer process behavior.

Proposition 4.5. *Assume that Hypotheses 2.1 and 2.2 hold. Let r and S_2^{in} be fixed. Let μ_1 and μ_2 be the specific growth rates defined in (4.2) and the set of the biological parameter values in Table 12. Let \mathcal{J}_i , $i = 0, \dots, 69$ be the various regions defined in Table 7. The existence and the local stability properties of steady states of the AM2 model with two interconnected chemostats (2.3) in the operating diagram are defined as follows:*

1. If $r \in (0, 1/2)$, $S_2^{in} > S_2^m$ and Case 1 of (4.1) holds ($m_1 > \mu_2(S_2^m)$), there are twenty-one regions \mathcal{J}_i , $i = 0 - 20$ shown in Figure 2.

2. If $r \in (0, 1/2)$, $S_2^{in} > S_2^m$ and Case 2 of (4.1) holds ($m_1 < \mu_2(S_2^{in})$), there are seventeen regions \mathcal{J}_i , $i = 0, 3 - 5, 8, 13 - 24$ shown in Figure 3.
3. If $r \in (0, 1/2)$, $S_2^{in} < S_2^m$ and Case 1 of (4.1) holds, there are twenty-one regions \mathcal{J}_i , $i = 0, 1, 4 - 9, 15 - 20, 25 - 31$ shown in Figure 4.
4. If $r \in (1/2, 1)$, $S_2^{in} > S_2^m$ and Case 1 of (4.1) holds, there are twenty regions \mathcal{J}_i , $i = 0, 15, 20 - 22, 32 - 46$ shown in Figure 5.

The conditions on the operating parameters defining the various boundaries of the regions are described in Table 13 [resp. Table 14] for the first three items [last item].

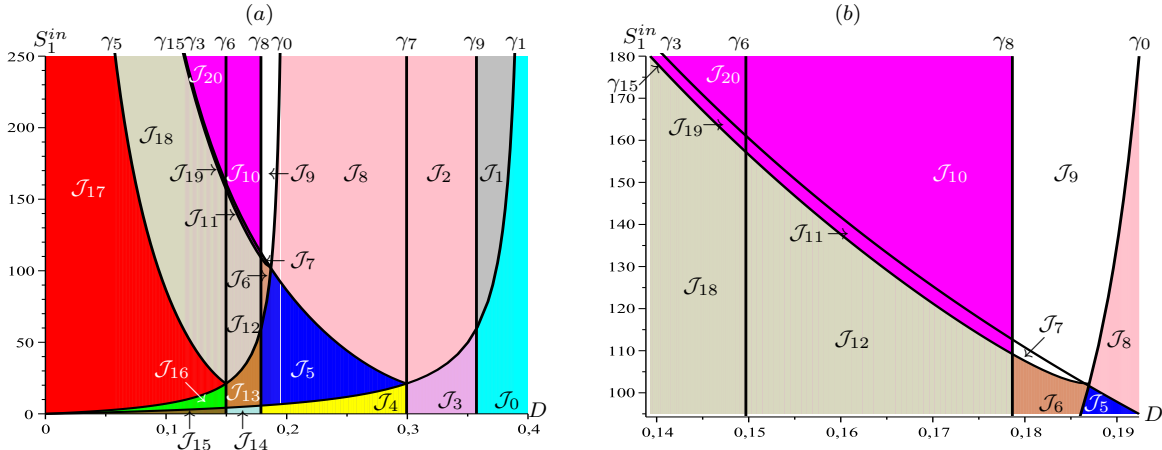


Figure 2. Operating diagram of (2.3) with twenty-one regions \mathcal{J}_i , $i = 0 - 20$ when $r = 1/3 \in (0, 1/2)$ and $S_2^{in} = 150 > S_2^m \approx 48.740$. Case 1 of (4.1): $m_1 = 0.6 > \mu_2(S_2^m) \approx 0.535$.

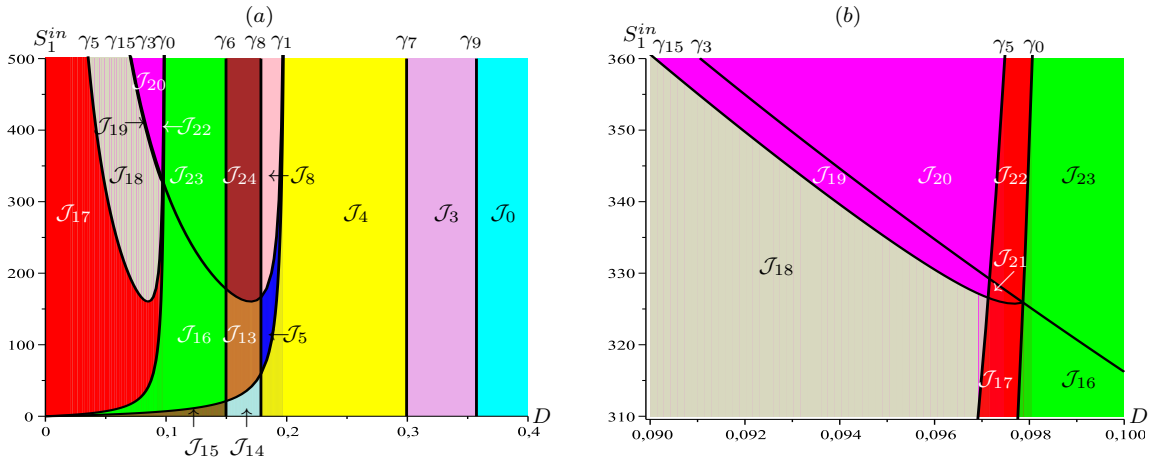


Figure 3. Operating diagram of (2.3) with seventeen regions \mathcal{J}_i , $i = 0, 3 - 5, 8, 13 - 24$ when $r = 1/3 \in (0, 1/2)$ and $S_2^{in} = 150 > S_2^m \approx 48.740$. Case 2 of (4.1): $m_1 = 0.3 < \mu_2(S_2^{in}) \approx 0.449$.

Note that we have chosen the same color for regions with the same number of LES steady states. For example, the regions \mathcal{J}_2 and \mathcal{J}_8 don't have the same number of unstable steady states, but they are colored in pink because both regions have the same behavior with the bistability between \mathcal{E}_{00}^{10} and \mathcal{E}_{00}^{11} (see Table 7). In summary, there are three types of behavior of the process: either the stability of only one steady state while all others are unstable if they exist; or the system exhibits bistability or the tristability of only two or three steady states while all others are unstable if they exist.

More precisely, the regions of existence of only one steady state LES (while all others are unstable if they exist) with the color are the following: \mathcal{E}_{00}^{00} in cyan (\mathcal{J}_0), \mathcal{E}_{00}^{10} in grey (\mathcal{J}_1), \mathcal{E}_{00}^{01} in yellow (\mathcal{J}_4), \mathcal{E}_{00}^{11} in blue ($\mathcal{J}_5, \mathcal{J}_{25}, \mathcal{J}_{64}$), \mathcal{E}_{10}^{11} in tan ($\mathcal{J}_6, \mathcal{J}_{63}, \mathcal{J}_{65}$), \mathcal{E}_{01}^{01} in sienna ($\mathcal{J}_{15}, \mathcal{J}_{35}, \mathcal{J}_{43}$), \mathcal{E}_{01}^{11} in green ($\mathcal{J}_{16}, \mathcal{J}_{23}, \mathcal{J}_{56}$), \mathcal{E}_{11}^{11} in red (\mathcal{J}_i , $i = 17, 21, 22, 30, 36, 37, 41, 42, 44 - 46, 62, 66$), \mathcal{E}_{10}^{10} in violet (\mathcal{J}_{32}).

Table 7

Existence and stability of steady states in the regions \mathcal{J}_i , $i = 0, \dots, 69$ of the operating diagrams in Figures 2 to 6.

	ε_{00}^{00}	ε_{00}^{01}	ε_{00}^{02}	ε_{00}^{10}	ε_{00}^{11}	ε_{00}^{12}	ε_{10}^{10}	ε_{10}^{11}	ε_{10}^{12}	ε_{01}^{01}	ε_{02}^{01}	ε_{01}^{11}	ε_{02}^{11}	ε_{11}^{11}	ε_{12}^{11}	Color
\mathcal{J}_0	S															Cyan
\mathcal{J}_1	U			S												Grey
\mathcal{J}_2	U	U	U	S	S	U										Pink
\mathcal{J}_3	S	S	U													Plum
\mathcal{J}_4	U	S														Yellow
\mathcal{J}_5	U	U		U	S											Blue
\mathcal{J}_6	U	U		U	U		U	S								Tan
\mathcal{J}_7	U	U		U	U		S	S	U							White
\mathcal{J}_8	U	U		S	S	U										Pink
\mathcal{J}_9	U	U		U	U	U	S	S	U							White
\mathcal{J}_{10}	U	U		U	U	U	S	S	U	U	U	U	U	S	U	Magenta
\mathcal{J}_{11}	U	U		U	U		S	S	U	U	U	U	U	S	U	Magenta
\mathcal{J}_{12}	U	U		U	U		U	S		U	U	U	U	S	U	Wheat
\mathcal{J}_{13}	U	U		U	S					U	U	S	U			Gold
\mathcal{J}_{14}	U	S								S	U					Turquoise
\mathcal{J}_{15}	U	U								S						Sienna
\mathcal{J}_{16}	U	U		U	U					U		S				Green
\mathcal{J}_{17}	U	U		U	U		U	U		U		U		S		Red
\mathcal{J}_{18}	U	U		U	U		U	S		U		U		S	U	Wheat
\mathcal{J}_{19}	U	U		U	U		S	S	U	U		U		S	U	Magenta
\mathcal{J}_{20}	U	U		U	U	U	S	S	U	U		U		S	U	Magenta
\mathcal{J}_{21}	U	U		U	U		U	U	U	U		U		S		Red
\mathcal{J}_{22}	U	U		U	U	U	U	U	U	U		U		S		Red
\mathcal{J}_{23}	U	U		U	U	U				U		S				Green
\mathcal{J}_{24}	U	U		S	S	U				U	U	S	U			Brown
\mathcal{J}_{25}	U			U	S											Blue
\mathcal{J}_{26}	U			S	S	U										Pink
\mathcal{J}_{27}	U	U		U	U	U	S	S	U					S	U	Magenta
\mathcal{J}_{28}	U	U		U	U		S	S	U		U		U	S	U	Magenta
\mathcal{J}_{29}	U	U		U	U		U	S						S	U	Wheat
\mathcal{J}_{30}	U	U		U	U		U	U						S		Red
\mathcal{J}_{31}	U	U		U	U		S	S								White
\mathcal{J}_{32}	U						S									Violet
\mathcal{J}_{33}	U						S			U	U			S	U	Navy
\mathcal{J}_{34}	S									S	U					Khaki
\mathcal{J}_{35}	U									S						Sienna
\mathcal{J}_{36}	U						U			U				S		Red
\mathcal{J}_{37}	U			U	U	U	U			U		U		S		Red
\mathcal{J}_{38}	U						S			U				S	U	Navy
\mathcal{J}_{39}	U			U	U	U	S			U		U		S	U	Navy
\mathcal{J}_{40}	U	U	U	U	U	U	S	S	U	U		U		S	U	Magenta
\mathcal{J}_{41}	U	U	U	U	U	U	U	U	U	U		U		S		Red
\mathcal{J}_{42}	U	U	U				U	U	U	U				S		Red
\mathcal{J}_{43}	U	U	U							S						Sienna
\mathcal{J}_{44}	U	U					U	U		U				S		Red
\mathcal{J}_{45}	U	U					U	U	U	U				S		Red
\mathcal{J}_{46}	U	U		U	U		U	U		U		U		S		Red
\mathcal{J}_{47}	S	S	U							S	U					Black
\mathcal{J}_{48}	U	U	U	U	S	U				U	U	S	U			Gold
\mathcal{J}_{49}	U	U	U	U	U	U	S	S	U	U	U	U	U	S	U	Magenta
\mathcal{J}_{50}	U	U		U	U	U	S	S	U	U	U	U	U	S	U	Magenta
\mathcal{J}_{51}	U	U		U	U		S	S	U	U	U	U	U	S	U	Magenta
\mathcal{J}_{52}	U	U		U	U		U	S		U	U	U	U	S	U	Wheat
\mathcal{J}_{53}	U	U		S	S	U				U	U	S	U			Coral
\mathcal{J}_{54}	U	U		U	S					U	U	S	U			Gold
\mathcal{J}_{55}	U	S								S	U					Turquoise
\mathcal{J}_{56}	U	U		U	U					U		S				Green
\mathcal{J}_{57}	U	U		U	U		U	S		U		U		S	U	Wheat
\mathcal{J}_{58}	U	U		U	U		S	S	U	U		U		S	U	Magenta
\mathcal{J}_{59}	U	U		U	U	U	S	S	U	U		U		S	U	Magenta
\mathcal{J}_{60}	U	U		U	U		S	S	U					S	U	Magenta
\mathcal{J}_{61}	U	U		U	U		U	S						S	U	Wheat
\mathcal{J}_{62}	U	U		U	U		U	U						S		Red
\mathcal{J}_{63}	U	U		U	U		U	S								Tan
\mathcal{J}_{64}	U			U	S											Blue
\mathcal{J}_{65}	U			U	U		U	S								Tan
\mathcal{J}_{66}	U			U	U		U	U						S		Red
\mathcal{J}_{67}	U			U	U		U	S						S	U	Wheat
\mathcal{J}_{68}	U			U	U		S	S	U					S	U	Magenta
\mathcal{J}_{69}	U			U	U	U	S	S	U					S	U	Magenta

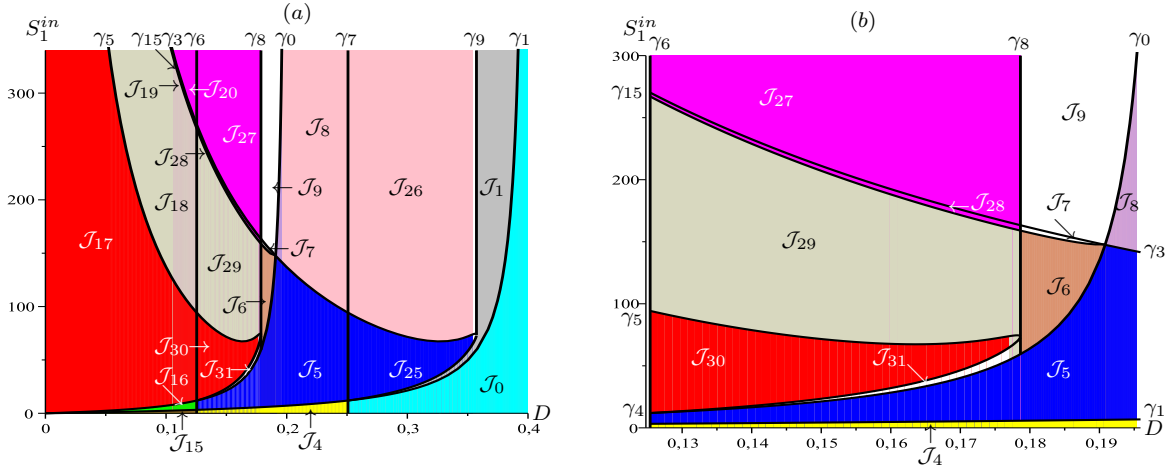


Figure 4. Operating diagram of (2.3) with twenty-one regions \mathcal{J}_i , $i = 0, 1, 4 - 9, 15 - 20, 25 - 31$ when $r = 1/3 \in (0, 1/2)$, and $S_2^{in} = 10 < S_2^m \approx 48.740$. Case 1 of (4.1): $m_1 = 0.6 > \mu_2(S_2^m) \approx 0.535$.

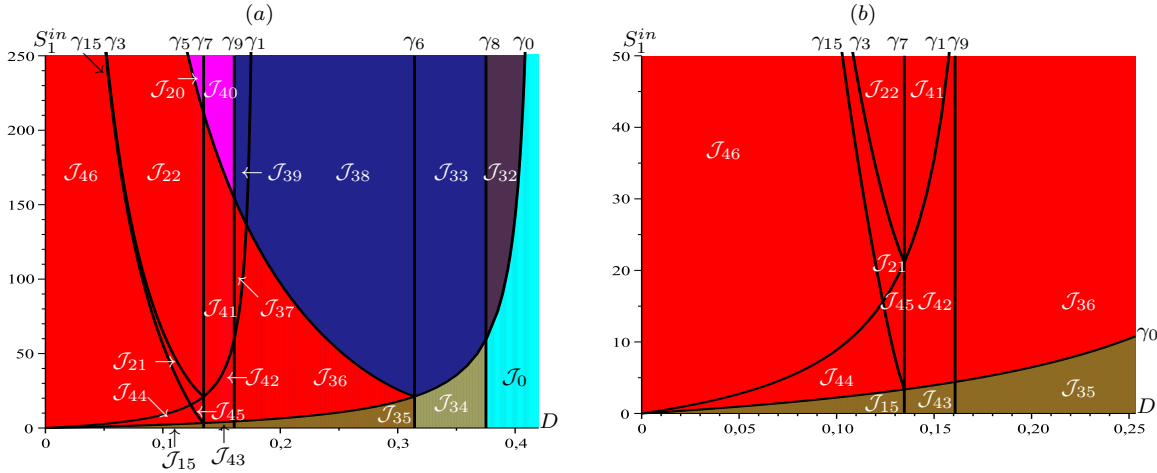


Figure 5. Operating diagram of (2.3) with twenty regions \mathcal{J}_i , $i = 0, 15, 20 - 22, 32 - 46$ when $r = 0.7 \in (1/2, 1)$ and $S_2^{in} = 150 > S_2^m \approx 48.740$. Case 1 of (4.1): $m_1 = 0.6 > \mu_2(S_2^m) \approx 0.535$.

The bistability regions with the corresponding two steady states LES (while all others are unstable if they exist) and color are the following: \mathcal{E}_{00}^{10} and \mathcal{E}_{00}^{11} in pink ($\mathcal{J}_2, \mathcal{J}_8, \mathcal{J}_{26}$), \mathcal{E}_{00}^{00} and \mathcal{E}_{00}^{01} in plum (\mathcal{J}_3), \mathcal{E}_{10}^{10} and \mathcal{E}_{10}^{11} in white ($\mathcal{J}_7, \mathcal{J}_9, \mathcal{J}_{31}$), \mathcal{E}_{10}^{11} and \mathcal{E}_{11}^{11} in wheat (\mathcal{J}_i , $i = 12, 18, 29, 52, 57, 61, 67$), \mathcal{E}_{00}^{11} and \mathcal{E}_{01}^{11} in gold ($\mathcal{J}_{13}, \mathcal{J}_{48}, \mathcal{J}_{54}$), \mathcal{E}_{00}^{01} and \mathcal{E}_{01}^{01} in turquoise ($\mathcal{J}_{14}, \mathcal{J}_{55}$), \mathcal{E}_{10}^{10} and \mathcal{E}_{11}^{11} in navy ($\mathcal{J}_{33}, \mathcal{J}_{38}, \mathcal{J}_{39}$), \mathcal{E}_{00}^{00} and \mathcal{E}_{01}^{01} in khaki (\mathcal{J}_{34}).

The tristability regions with the corresponding three steady states LES and color are the following: \mathcal{E}_{10}^{10} , \mathcal{E}_{10}^{11} and \mathcal{E}_{11}^{11} in magenta (\mathcal{J}_i , $i = 10, 11, 19, 20, 27, 28, 40, 49 - 51, 58 - 60, 68, 69$), \mathcal{E}_{00}^{10} , \mathcal{E}_{00}^{11} and \mathcal{E}_{01}^{11} in brown (\mathcal{J}_{24}), \mathcal{E}_{00}^{00} , \mathcal{E}_{00}^{01} and \mathcal{E}_{01}^{01} in black (\mathcal{J}_{47}), \mathcal{E}_{00}^{10} , \mathcal{E}_{00}^{11} and \mathcal{E}_{01}^{11} in coral (\mathcal{J}_{53}).

4.2. . Operating diagrams in the plane (S_2^{in}, S_1^{in}) when D and r are fixed.

Proposition 4.6. For D fixed in $(0, r\mu_2(S_2^m))$ and $r \in (0, 1)$, the lines γ_0 , γ_4 and γ_{10} intersect at the same point $(S_{21}^{in*}, \lambda_1^1(D, r))$. In addition, the lines γ_0 , γ_5 and γ_{12} intersect at the same point $(S_{23}^{in*}, \lambda_1^1(D, r))$ in the plane (S_2^{in}, S_1^{in}) , where $S_{21}^{in*} = \lambda_2^{11}(D, r)$ and $S_{23}^{in*} = \lambda_2^{12}(D, r)$ (see Figure 6). Moreover:

- If $S_2^{in} < S_{21}^{in*}$, then $\lambda_1^1(D, r) < F_{11}(D, r, S_2^{in}) < F_{12}(D, r, S_2^{in})$.
- If $S_{21}^{in*} < S_2^{in} < S_{23}^{in*}$, then $F_{11}(D, r, S_2^{in}) < \lambda_1^1(D, r) < F_{12}(D, r, S_2^{in})$.
- If $S_2^{in} > S_{23}^{in*}$, then $F_{11}(D, r, S_2^{in}) < F_{12}(D, r, S_2^{in}) < \lambda_1^1(D, r)$.

For D fixed in $(0, r_2\mu_2(S_2^m))$ and $r \in (0, 1)$, the lines γ_1 , γ_2 , γ_{11} intersect at the same point $(S_{22}^{in*}, \lambda_1^2(D, r))$ and the lines γ_1 , γ_3 , γ_{13} intersect at the same point $(S_{24}^{in*}, \lambda_1^2(D, r))$ in the plane (S_2^{in}, S_1^{in}) , where $S_{22}^{in*} = \lambda_2^{21}(D, r)$ and $S_{24}^{in*} = \lambda_2^{22}(D, r)$ (see Figure 6). Moreover:

- If $S_2^{in} < S_{22}^{in*}$, then $\lambda_1^2(D, r) < F_{21}(D, r, S_2^{in}) < F_{22}(D, r, S_2^{in})$.

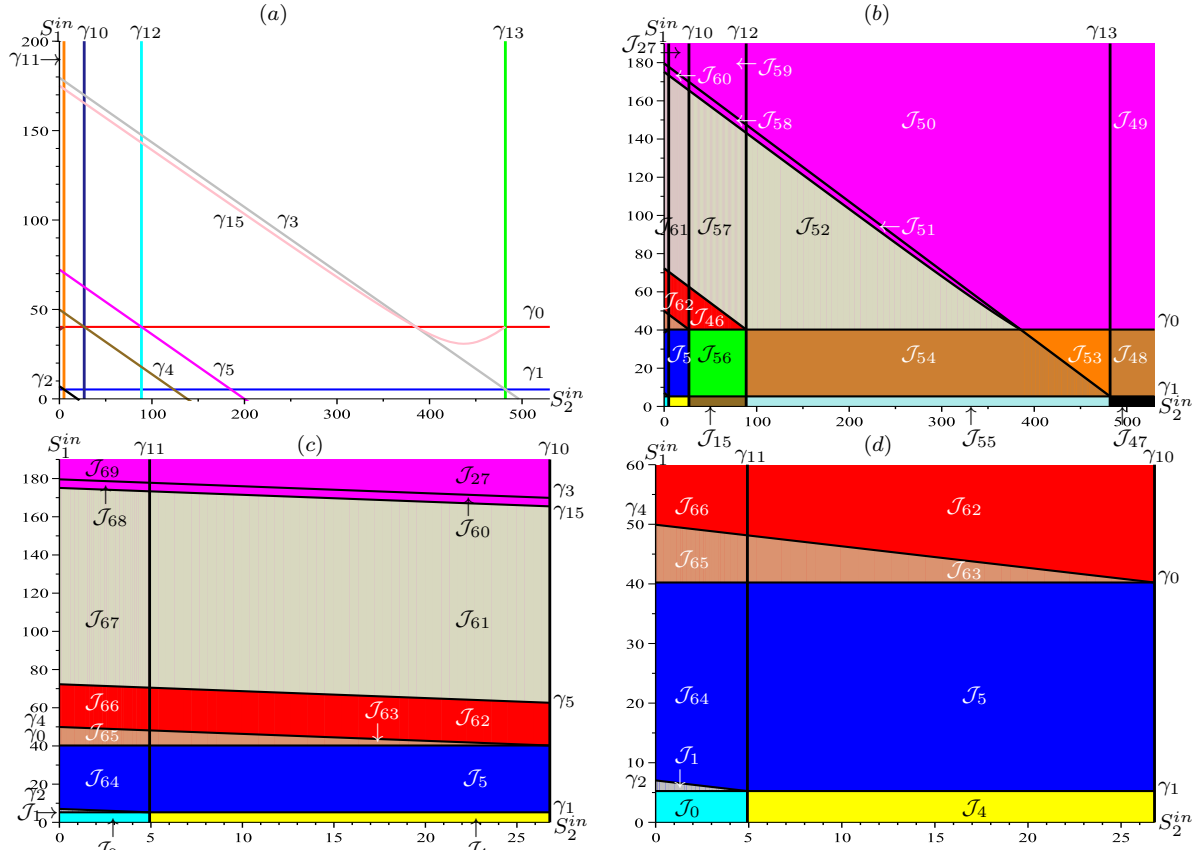


Figure 6. Operating diagram of (2.3) in the plane (S_2^{in}, S_1^{in}) with thirty regions \mathcal{J}_i , $i = 0, 1, 4, 5, 15, 27, 46 - 69$ when $D = 0.17$ and $r = 0.3 \in (0, 1/2)$.

- If $S_{24}^{in*} < S_2^{in} < S_{24}^{in*}$, then $F_{21}(D, r, S_2^{in}) < \lambda_1^2(D, r) < F_{22}(D, r, S_2^{in})$.
- If $S_2^{in} > S_{24}^{in*}$, then $F_{21}(D, r, S_2^{in}) < F_{22}(D, r, S_2^{in}) < \lambda_1^2(D, r)$.

Proposition 4.7. Assume that *Hypotheses 2.1* and *2.2* hold. Let r and D be fixed so that $0 < r < 1/2$ and $D \in (0, \mu_2(S_2^m))$. For the specific growth rates μ_1 and μ_2 defined in (4.2) and the set of the biological parameter values in Table 12, the existence and the local stability properties of steady states of system (2.3) in the thirty regions \mathcal{J}_i , $i = 0, 1, 4, 5, 15, 27, 46 - 69$ of the operating diagram shown in Figure 6 are defined in Table 7, where the conditions on the operating parameters defining the various boundaries of the regions are described in Table 15.

5. Discussion and conclusion. In this paper, we have introduced the original AM2 model (2.3) with a serial configuration of two chemostats, thanks to the mass conservation principle. The mathematical model considered is a differential system in eight dimensions. The analysis of this model is original and has not been studied in the literature. Using the same dilution rate with a large class of monotonic and nonmonotonic growth functions for the first and the second species, we have presented an in-depth mathematical study of system (2.3). Since this model has a cascade structure, we show that it can be reduced to a four-dimensional system (3.2). The existence and the stability of each steady state of the complete model (2.3) can be deduced from the reduced model (3.2). The necessary and sufficient conditions of existence and local stability of all steady states of (3.2) are established according to the four operating parameters D , r , S_1^{in} and S_2^{in} . Generically, there can be nine types of steady states, six of which can be doubled for non-monotonic growth rates, giving a total of fifteen steady states.

To describe the behavior of the process when these four control parameters are varied, we have determined theoretically the operating diagram from the existence and local stability conditions. Fixing the biological parameter set provided in Table 12, there can be seventy regions with three different behaviors: either the stability of a single LES steady state, or bistability or

tristability, with the existence of two or three stable steady states, while all other steady states are unstable when they exist.

It is interesting to note that this general study includes in fact a number of already known results. In other words, the actual results comprise results that were already established for specific functioning conditions. In particular, it is the case when the functioning conditions are such that both biomasses are washed in the first reactor (i.e. when $X_1^1 = 0$ and $X_2^1 = 0$): the results obtained are then equivalent to those obtained for the analysis of the AM2 model considered in a single chemostat [5, 41]. It is logically the case when the first reactor is smaller than the first one, in which case, for a given too high dilution rate, the washout of the biomasses arises in the first reactor. The other singular case is that one in which the first biomass is washed out in both reactors: in such a case the analysis is equivalent to the study of a single bioreaction i) having as bioreactional scheme $S_2 \rightarrow X_2 + \text{biogas}$ and ii) taking place in a system of two chemostats in series [9, 11]. Following the same idea, we also find more recent results established in [25]. These authors had shown that under certain circumstances, well characterized as a function of operating conditions and system parameters by Sari and Benyahia (cf. [41]), a multi-step system (in the sense that the substrate feed to a reaction i is the reaction output of step $i - 1$, which is the case of the AM2 reaction scheme), in a chemostat could exhibit highly original behavior. In particular, it was shown that in these particular circumstances, the system can be stabilized by increasing the feed rate, rather than decreasing it as is traditionally the case. It's interesting to note that this is the case here for two chemostats in series, and it may happen when the value of r is smaller than $1/2$. In fact it appears that the operating diagrams shown in Figures 3 and 4, were drawn up with values that allow these results to be found. Consider Figure 3 where $S_2^{in} > S_2^m$ and Case 1 of (4.1) ($m_1 > \mu_2(S_2^m)$) holds: the red zone rises slightly to the right of the lowest point of the wheat zone. Let's start from a point in the wheat zone, very close to its low point. In this zone (denoted \mathcal{J}_{18} in Figure 3), there are two stable steady states. Suppose that the initial conditions are such that the system converges to the steady state \mathcal{E}_{10}^{11} characterized by $X_2^1 = 0$. We can imagine that on an operational level, it is not desirable to have one of the biomasses of the first reactor which is zero. By increasing D very slightly, we will find ourselves in the part of the red zone (\mathcal{J}_{17}) which goes up to the right of the low point of the wheat zone. In other words, we find ourselves in a zone where the only stable steady state is now the positive steady state \mathcal{E}_{11}^{11} , having increased rather than decreased the feed rate of the system!

Now, when $r < 1/2$, $S_2^{in} < S_2^m$ and Case 2 of (4.1) ($m_1 < \mu_2(S_2^{in})$) holds, one has exactly the same phenomenon that can be highlighted from the operating diagram plotted in Figure 4.

To enhance and extend the results of the mathematical study of this anaerobic digestion process with a series configuration of interconnected chemostats, a forthcoming paper will analyse performance criteria by comparing with the single chemostat.

Appendix A. Proofs. First, we need the following Lemmas to establish the existence and multiplicity of all steady states of (3.2).

Lemma A.1. *Let f_1 and g_1 be the functions defined in Table 2. Let $X_1^{1*} < S_1^{in}/k_1$. Assume that Hypothesis 2.1 holds. The equation $f_1(x) = g_1(x)$ has a unique solution in $(X_1^{1*}, S_1^{in}/k_1)$ (see Figure 7(a)).*

Proof of Lemma A.1. Under Hypothesis 2.1, the function $x \mapsto f_1(x)$ is nonnegative, decreasing and continuous on $[0, S_1^{in}/k_1]$. The function $x \mapsto g_1(x)$ is nonnegative, increasing hyperbola and continuous on $[X_1^{1*}, +\infty)$. Indeed,

$$g_1'(x) = D_2 \frac{X_1^{1*}}{x^2} > 0.$$

Let $X_1^{1*} < S_1^{in}/k_1$ and F_1 be the function defined by $F_1(x) := f_1(x) - g_1(x)$. Therefore, F_1 is

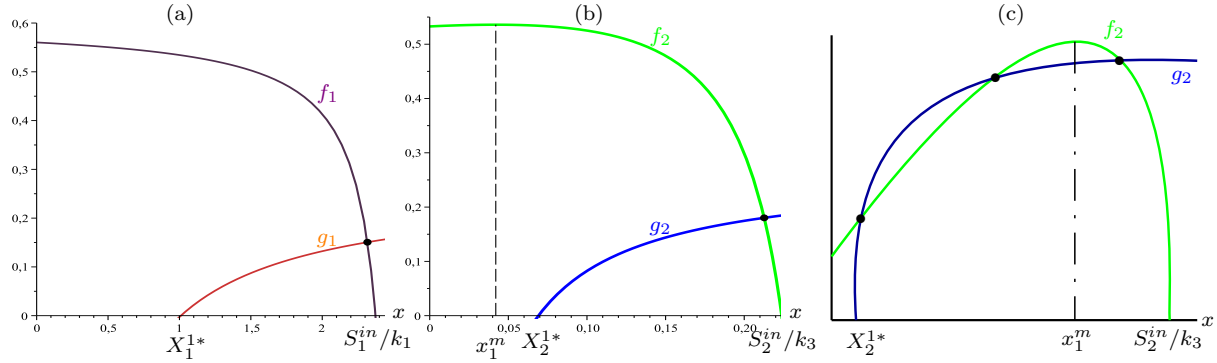


Figure 7. Number of positive solutions of equations : (a) $f_1(x) = g_1(x)$ (unique solution); (b) $f_2(x) = g_2(x)$ (unique solution when $X_2^{1*} \geq x_1^m$); (c) $f_2(x) = g_2(x)$ (an odd number of intersections when $X_2^{1*} < x_1^m$).

decreasing continuous on $[X_1^{1*}, S_1^{in}/k_1]$. In addition, we have

$$F_1(X_1^{1*}) = \mu_1(S_1^{in} - k_1 X_1^{1*}) > 0 \quad \text{and} \quad F_1\left(\frac{S_1^{in}}{k_1}\right) = -g_1\left(\frac{S_1^{in}}{k_1}\right) < 0.$$

Using the Intermediate Value Theorem, it follows that the equation $F_1(x) = 0$ has a unique solution in $(X_1^{1*}, S_1^{in}/k_1)$ (see Figure 7(a)). ■

Lemma A.2. Let f_2 and g_2 be the functions defined in Table 2. Let X_2^{1*} be a positive constant so that $X_2^{1*} < S_2^{in}/k_3$ and $x_1^m := (S_2^{in} - S_2^m)/k_3$ be the maximum value of f_2 on $[0, S_2^{in}/k_3]$. Assume that Hypothesis 2.2 holds.

1. When $X_2^{1*} \geq x_1^m$, then the equation $f_2(x) = g_2(x)$ has a unique solution in $(X_2^{1*}, S_2^{in}/k_3)$, (see Figure 7(b)).
2. When $X_2^{1*} < x_1^m$ then the equation $f_2(x) = g_2(x)$ has at least one solution in $(X_2^{1*}, S_2^{in}/k_3)$. Generically, there exist an odd number of solutions in $(X_2^{1*}, S_2^{in}/k_3)$, (see Figure 7(c)).

Proof of Lemma A.2. Under Hypothesis 2.2, f_2 is nonnegative and continuous on the interval $[0, S_2^{in}/k_3]$. In addition, f_2 is increasing on $[0, x_1^m]$ and is decreasing on $[x_1^m, S_2^{in}/k_3]$. The function g_2 is nonnegative and increasing hyperbola continuous on $[X_2^{1*}, +\infty)$. Indeed,

$$(A.1) \quad g_2'(x) = D_2 \frac{X_2^{1*}}{x^2} > 0.$$

Let $X_2^{1*} < S_2^{in}/k_3$ and let F_2 be the function defined by $F_2(x) := f_2(x) - g_2(x)$. Therefore, F_2 is continuous on $[X_2^{1*}, S_2^{in}/k_3]$. In addition, we have

$$F_2(X_2^{1*}) = \mu_2(S_2^{in} - k_3 X_2^{1*}) > 0 \quad \text{and} \quad F_2\left(\frac{S_2^{in}}{k_3}\right) = -g_2\left(\frac{S_2^{in}}{k_3}\right) < 0.$$

If $X_2^{1*} > x_1^m$ then F_2 is decreasing on $[X_2^{1*}, S_2^{in}/k_3]$, because f_2 is decreasing and g_2 is increasing on the same interval. Consequently, the equation $F_2(x) = 0$ has a unique solution on $(X_2^{1*}, S_2^{in}/k_3)$, (see Figure 7(b)). If $X_2^{1*} < x_1^m$, then F_2 can be nonmonotonic. We complete the proof by using the Intermediate Value Theorem. ■

Lemma A.3. Let f_3 and g_2 be the functions defined in Table 2. Let $d := (S_2^{in} + k_2 X_1^{2*})/k_3$ be the root of $f_3(x) = 0$ and $x_2^m := (S_2^{in} + k_2 X_1^{2*} - S_2^m)/k_3$ be the maximum value of f_3 . Assume that $X_2^{1*} < d$ and Hypothesis 2.2 holds.

1. When $X_2^{1*} \geq x_2^m$ then the equation $f_3(x) = g_2(x)$ has a unique solution in (X_2^{1*}, d) (see Figure 8(a)).
2. When $X_2^{1*} < x_2^m$ then the equation $f_3(x) = g_2(x)$ has at least one solution in (X_2^{1*}, d) . Generically, there exist an odd number of solutions in (X_2^{1*}, d) , (see Figure 8(b-c)).

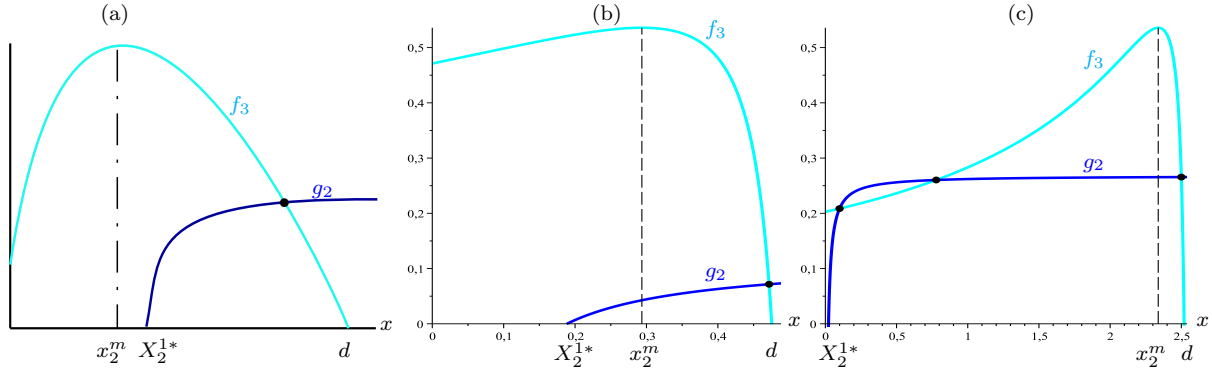


Figure 8. Number of positive solutions of equation $f_3(x) = g_2(x)$ on $(0, d)$ where d is defined in [Lemma A.3](#): (a) unique solution when $X_2^{1*} \geq x_2^m$; (b-c) an odd number of intersections when $X_2^{1*} < x_2^m$.

Proof of Lemma A.3. Under [Hypothesis 2.2](#), f_3 is nonnegative and continuous on $[0, d]$ with $d := (S_2^{in} + k_2 X_1^{2*})/k_3$. In addition, f_3 is increasing on $[0, x_2^m]$ and is decreasing on $[x_2^m, d]$. Let $X_2^{1*} < d$ and F_3 be the function defined by $F_3(x) := f_3(x) - g_2(x)$. Therefore, F_3 is continuous on $[X_2^{1*}, d]$. In addition, we have

$$F_3(X_2^{1*}) = \mu_2(S_2^{in} + k_2 X_1^{2*} - k_3 X_2^{1*}) > 0, \quad F_3\left(\frac{S_2^{in} + k_2 X_1^{2*}}{k_3}\right) = -g_2\left(\frac{S_2^{in} + k_2 X_1^{2*}}{k_3}\right) < 0.$$

Recall from [\(A.1\)](#) that g_2 is increasing on $[X_2^{1*}, +\infty)$. If $X_2^{1*} \geq x_2^m$ then F_3 is decreasing on $[X_2^{1*}, d]$, because f_3 is decreasing on the same interval. Consequently, the equation $F_3(x) = 0$ has a unique solution in (X_2^{1*}, d) . If $X_2^{1*} < x_2^m$ then F_3 can be nonmonotonic. Using the Intermediate Value Theorem, the proof is completed. ■

Proof of Proposition 3.1. Similarly to system [\(2.2\)](#), subsystem [\(3.2\)](#) has a cascade structure. Thus, for each steady state of the upper two-dimensional system of [\(3.2\)](#) denoted by

$$E_{ij}(X_1^1, X_2^1), \quad \{i, j\} \in \{0, 1, 2\}$$

corresponds a steady state of the lower two-dimensional system of [\(3.2\)](#) denoted by

$$E_{ij}^{kl}(X_1^2, X_2^2).$$

This steady state is given by putting the left-hand side of the lower two-dimensional subsystem of [\(3.2\)](#) equal to zero when the two components X_1^1 and X_2^1 are at the steady state E_{ij} . Then, we can deduce the corresponding steady state of the four-dimensional system [\(3.2\)](#) denoted by $\mathcal{E}_{ij}^{kl}(X_1^1, X_2^1, X_1^2, X_2^2)$ as well as their existence condition by checking those of E_{ij} and E_{ij}^{kl} simultaneously. Indeed, the upper two-dimensional system of [\(3.2\)](#) corresponds to the classic AM2 model where the steady states are given by the solutions of the following equations:

$$(A.2) \quad [\mu_1(S_1^{in} - k_1 X_1^1) - D_1] X_1^1 = 0,$$

$$(A.3) \quad [\mu_2(S_2^{in} + k_2 X_1^1 - k_3 X_2^1) - D_1] X_2^1 = 0.$$

- For E_{00} , $X_1^1 = X_2^1 = 0$. It always exists.
- For E_{10} , $X_1^1 > 0$ and $X_2^1 = 0$. Thus, [\(A.2\)](#) results in $\mu_1(S_1^{in} - k_1 X_1^1) = D/r$. Using [Hypothesis 2.1](#), we obtain X_1^1 and the existence condition in [Table 8](#).
- For E_{0i} , $i = 1, 2$, $X_1^1 = 0$ and $X_2^1 > 0$. Hence, [\(A.3\)](#) results in $\mu_2(S_2^{in} - k_3 X_2^1) = D/r$. Using [Hypothesis 2.2](#), we obtain X_2^1 and the existence condition in [Table 8](#).
- For E_{1i} , $i = 1, 2$, $X_1^1 > 0$ and $X_2^1 > 0$. From [\(A.2\)](#) and [\(A.3\)](#), it follows that

$$\mu_1(S_1^{in} - k_1 X_1^1) = D_1 \quad \text{and} \quad \mu_2(S_2^{in} + k_2 X_1^1 - k_3 X_2^1) = D_1.$$

Table 8

Two components (X_1^1, X_2^1) of all steady states and their existence condition for the upper two-dimensional system of (3.2). The functions λ_1^1 , λ_2^1 , and F_{1i} , $i = 1, 2$ are defined in Table 1.

	X_1^1	X_2^1	Existence conditions
E_{00}	0	0	Always exists
E_{10}	$\frac{1}{k_1} (S_1^{in} - \lambda_1^1)$	0	$S_1^{in} > \lambda_1^1$
E_{0i}	0	$\frac{1}{k_3} (S_2^{in} - \lambda_2^i)$	$S_2^{in} > \lambda_2^i$
E_{1i}	$\frac{1}{k_1} (S_1^{in} - \lambda_1^1)$	$\frac{k_2}{k_1 k_3} (S_1^{in} - F_{1i})$	$S_1^{in} > \lambda_1^1$ and $S_1^{in} > F_{1i}$

Using the expressions of λ_1^1 , λ_2^1 , and F_{1i} , $i = 1, 2$ in Table 1, we obtain the two components of E_{1i} and the two existence conditions in Table 8.

The steady states of the lower two-dimensional system of (3.2) are given by the solutions of the following equations:

$$(A.4) \quad \mu_1 (S_1^{in} - k_1 X_1^2) X_1^2 + D_2 (X_1^1 - X_1^2) = 0,$$

$$(A.5) \quad \mu_2 (S_2^{in} + k_2 X_1^2 - k_3 X_2^2) X_2^2 + D_2 (X_2^1 - X_2^2) = 0.$$

Table 9

Two components (X_1^2, X_2^2) and existence condition of all steady states of the lower two-dimensional system of (3.2). The functions λ_1^2 , λ_2^2 , and F_{2i} , $i = 1, 2$ are defined in Table 1. The functions f_1 , f_2 , f_3 , g_1 and g_2 are defined in Table 2 while X_1^{2*} is the unique solution of equation $f_1(x) = g_1(x)$.

	X_1^2	X_2^2	Existence conditions
E_{00}^{00}	0	0	Always exists
E_{00}^{10}	$\frac{1}{k_1} (S_1^{in} - \lambda_1^2)$	0	$S_1^{in} > \lambda_1^2$
E_{00}^{0i}	0	$\frac{1}{k_3} (S_2^{in} - \lambda_2^i)$	$S_2^{in} > \lambda_2^i$
E_{00}^{1i}	$\frac{1}{k_1} (S_1^{in} - \lambda_1^2)$	$\frac{k_2}{k_1 k_3} (S_1^{in} - F_{2i})$	$S_1^{in} > \lambda_1^2$ and $S_1^{in} > F_{2i}$
E_{10}^{10}	X_1^{2*}	0	Always exists
E_{10}^{1i}	X_1^{2*}	$\frac{1}{k_3} (S_2^{in} + k_2 X_1^{2*} - \lambda_2^i)$	$S_2^{in} + k_2 X_1^{2*} > \lambda_2^i$
E_{0i}^{01}	0	a solution of $f_2(X_2^2) = g_2(X_2^2)$	Always exists
E_{0i}^{11}	$\frac{1}{k_1} (S_1^{in} - \lambda_1^2)$	a solution of $f_3(x) = g_2(x)$	$S_1^{in} > \lambda_1^2$
E_{1i}^{11}	X_1^{2*}	a solution of $f_3(x) = g_2(x)$	Always exists

- For E_{00} , we have $X_1^1 = X_2^1 = 0$. Hence, (A.4) and (A.5) result in

$$(A.6) \quad [\mu_1 (S_1^{in} - k_1 X_1^2) - D_2] X_1^2 = 0,$$

$$(A.7) \quad [\mu_2 (S_2^{in} + k_2 X_1^2 - k_3 X_2^2) - D_2] X_2^2 = 0.$$

- For E_{00}^{00} , $X_1^2 = X_2^2 = 0$. It always exists.
- For E_{00}^{10} , $X_1^2 > 0$ and $X_2^2 = 0$. Thus, (A.6) results in $\mu_1 (S_1^{in} - k_1 X_1^2) = D/(1-r)$. Using Hypothesis 2.1, we obtain X_1^2 and the existence condition in Table 9.
- For E_{00}^{0i} , $i = 1, 2$, $X_1^2 = 0$ and $X_2^2 > 0$. Hence, (A.7) results in $\mu_2 (S_2^{in} - k_3 X_2^2) = D/(1-r)$. Using Hypothesis 2.2, we obtain X_2^2 and the existence condition in Table 9.
- For E_{00}^{1i} , $i = 1, 2$, $X_1^2 > 0$ and $X_2^2 > 0$. Thus, (A.6) and (A.7) result in

$$\mu_1 (S_1^{in} - k_1 X_1^2) = D_2 \quad \text{and} \quad \mu_2 (S_2^{in} + k_2 X_1^2 - k_3 X_2^2) = \frac{D}{1-r}.$$

Using Hypotheses 2.1 and 2.2 and the expressions of λ_1^2 , λ_2^2 , and F_{2i} in Table 1, we obtain two components (X_1^2, X_2^2) and the two existence conditions in Table 9.

- For E_{10} , we have $X_1^1 > 0$ and $X_2^1 = 0$. Hence, (A.4) and (A.5) result in

$$(A.8) \quad \mu_1 (S_1^{in} - k_1 X_1^2) X_1^2 + D_2 (X_1^1 - X_1^2) = 0,$$

$$(A.9) \quad [\mu_2 (S_2^{in} + k_2 X_1^2 - k_3 X_2^2) - D_2] X_2^2 = 0.$$

- For E_{10}^{00} , $X_1^2 = X_2^2 = 0$. Then (A.8) implies that $X_1^1 = 0$, which is in contradiction with the existence condition of E_{10} where $X_1^1 > 0$. Hence, E_{10}^{00} does not exist.
- For E_{10}^{10} , $X_1^2 > 0$ and $X_2^2 = 0$. Thus, (A.8) results in

$$(A.10) \quad \mu_1 (S_1^{in} - k_1 X_1^2) = D_2 \left(\frac{X_1^2 - X_1^1}{X_1^2} \right),$$

which is equivalent to $f_1(x) = g_1(x)$ (see Table 2). From the component X_1^1 of E_{10} in Table 8, it follows that $X_1^1 < S_1^{in}/k_1$. From Lemma A.1, it follows that the equation $f_1(x) = g_1(x)$ has a unique solution $X_1^{2*} \in (X_1^1, S_1^{in}/k_1)$ (see Figure 7(a)). Thus, we obtain the components of steady state E_{10}^{10} in Table 9, which always exists.

- For E_{10}^{0i} , $i = 1, 2$, $X_1^2 = 0$ and $X_2^2 > 0$. Then (A.8) implies that $X_1^1 = 0$, which is in contradiction with the existence condition of E_{10} where $X_1^1 > 0$. Hence, E_{10}^{0i} does not exist.
- For E_{10}^{1i} , $i = 1, 2$, $X_1^2 > 0$ and $X_2^2 > 0$. Thus, (A.8) is equivalent to (A.10). Similarly to the steady state E_{10}^{10} , equation (A.10) has a unique solution $X_1^{2*} \in (X_1^1, S_1^{in}/k_1)$. In addition, (A.9) implies that

$$\mu_2 (S_2^{in} + k_2 X_1^{2*} - k_3 X_2^2) = D_2.$$

From Hypothesis 2.2 and the expression of λ_2^{2i} in Table 1, we obtain the component X_2^2 of the steady state E_{10}^{1i} in Table 9. Moreover, the existence condition in Table 9 follows.

- For E_{0i} , we have $X_1^1 = 0$ and $X_2^{1i} > 0$, $i = 1, 2$. Hence, (A.4) and (A.5) result in

$$(A.11) \quad [\mu_1 (S_1^{in} - k_1 X_1^2) - D_2] X_1^2 = 0,$$

$$(A.12) \quad \mu_2 (S_2^{in} + k_2 X_1^2 - k_3 X_2^2) X_2^2 + D_2 (X_2^{1i} - X_2^2) = 0.$$

- For E_{0i}^{00} [resp. E_{0i}^{10}], $X_1^2 = X_2^2 = 0$ [resp. $X_1^2 > 0$ and $X_2^2 = 0$]. Then (A.12) implies that $X_2^{1i} = 0$, which is in contradiction with $X_2^{1i} > 0$. Hence, E_{0i}^{00} and E_{0i}^{10} does not exist.
- For E_{0i}^{01} , we have $X_1^2 = 0$ and $X_2^2 > 0$. Then, (A.12) results in X_2^2 must be a solution of equation

$$\mu_2 (S_2^{in} - k_3 X_2^2) = D_2 \left(\frac{X_2^2 - X_2^{1i}}{X_2^2} \right),$$

which is equivalent to $f_2(X_2^2) = g_2(X_2^2)$ (see Table 2). From the component X_2^{1i} of E_{0i} in Table 8, we have $X_2^{1i} < S_2^{in}/k_3$. From Lemma A.2, it follows that the equation $f_2(X_2^2) = g_2(X_2^2)$ has at least one solution $X_2^{2*} \in (X_2^{1i}, S_2^{in}/k_3)$. Hence, we obtain the components of steady state E_{0i}^{01} in Table 9, where there exists at least one.

- For E_{0i}^{11} , we have $X_1^2 > 0$ and $X_2^2 > 0$. Then, the component X_1^2 in Table 9 follows from equation (A.11) and Hypothesis 2.1. In addition, (A.12) implies that X_2^2 must be a solution of equation

$$(A.13) \quad \mu_2 (S_2^{in} + k_2 X_1^2 - k_3 X_2^2) = D_2 \left(\frac{X_2^2 - X_2^{1i}}{X_2^2} \right),$$

which is equivalent to $f_3(X_2^2) = g_2(X_2^2)$ (see Table 2). Using the expression of d in Lemma A.3 and the component of X_2^{1i} in Table 8, we see that $X_2^{1i} < d$. From Lemma A.3, it follows that the equation $f_3(X_2^2) = g_2(X_2^2)$ has at least one solution $X_2^{2*} \in (X_2^{1i}, d)$ (see Figure 8). Consequently, we obtain the two components and the existence condition of the steady state E_{0i}^{11} in Table 9.

- For E_{1i} , we have $X_1^1 > 0$ and $X_2^{1i} > 0$, $i = 1, 2$.
 - For E_{1i}^{00} [resp. E_{1i}^{10} , and E_{1i}^{01}], $X_1^2 = X_2^2 = 0$ [resp. $(X_1^2 > 0$ and $X_2^2 = 0)$ and $(X_1^2 = 0$ and $X_2^2 > 0)$]. Then, (A.4) or (A.5) implies that $X_1^1 = 0$ or $X_2^{1i} = 0$, which is a contradiction. Hence, these three types of steady states do not exist.
 - For E_{1i}^{11} , we have $X_1^2 > 0$ and $X_2^2 > 0$. Then, (A.4) and (A.5) are equivalent to (A.10) and (A.13), or, equivalently, $f_1(x) = g_1(x)$ and $f_3(x) = g_2(x)$, respectively. Similarly to the steady state E_{10}^{10} , we obtain the component X_1^2 which is the unique solution of equation $f_1(x) = g_1(x)$. Using the expression of X_1^{1*} and X_2^{1i*} in Table 8 and the expressions of F_{1i} in Table 1, it follows that

$$X_2^{1i*} = \frac{1}{k_3} (k_2 X_1^{1*} - \lambda_2^{1i} + S_2^{in}).$$

From the expressions of d in Lemma A.3, we have

$$X_2^{1i*} - d = \frac{1}{k_3} (k_2 (X_1^{1*} - X_1^{2*}) - \lambda_2^{1i}),$$

which is negative since $X_1^{1*} < X_1^{2*}$ (see Lemma A.1). From Lemma A.3, it follows that the equation $f_3(x) = g_2(x)$ has at least one solution in (X_2^{1i*}, d) . Therefore, we obtain the two components of the steady state E_{1i}^{11} in Table 9, which always exists. ■

Proof of Proposition 3.2. For $k = 0, 1$ and $l = 0, 1, 2$, the uniqueness of the six first steady states \mathcal{E}_{00}^{kl} and \mathcal{E}_{10}^{ll} , follows from Table 3. For \mathcal{E}_{01}^{01} , we have $\lambda_2^{11} < S_2^m$, that is, $X_2^{1*} > (S_2^{in} - S_2^m) / k_3 := x_1^m$ where X_2^{1*} is defined in Table 3 and x_1^m in Lemma A.2, implying that the equation $f_2(X_2^2) = g_2(X_2^2)$ has a unique solution in $(X_2^{1*}, S_2^{in}/k_3)$ (see Figure 7(b)). That is, \mathcal{E}_{01}^{01} is unique when it exists. Inversely, for \mathcal{E}_{02}^{01} , we have $\lambda_2^{12} > S_2^m$, that is, $X_2^{1*} < x_1^m$. From Lemma A.2, the equation $f_2(X_2^2) = g_2(X_2^2)$ has at least one solution on $(X_2^{1*}, S_2^{in}/k_3)$ (see Figure 7(b-c)). For \mathcal{E}_{0i}^{11} , $i = 1, 2$, the X_2^2 -component is a solution of $f_3(x) = g_2(x)$. Using the expressions of X_2^{1*} and X_1^{2*} in Table 3 and the expressions of x_2^m in Lemma A.3, a straightforward calculation shows that

$$X_2^{1*} - x_2^m = \frac{1}{k_3} \left(S_2^m - \lambda_2^{11} - \frac{k_2}{k_1} (S_1^{in} - \lambda_1^2) \right).$$

As $S_2^m > \lambda_2^{11}$ and $S_1^{in} > \lambda_1^2$, the two case $X_2^{1*} \geq x_2^m$ and $X_2^{1*} < x_2^m$ can be hold. From Lemma A.3, the equation $f_3(x) = g_2(x)$ has at least one solution in (X_2^{1*}, d) (see Figure 8). The multiplicity of the other steady states \mathcal{E}_{11}^{11} and \mathcal{E}_{12}^{12} follows similar arguments. ■

Proof of Proposition 3.3. Let J be the Jacobian matrix of (3.2) at $(X_1^1, X_2^1, X_1^2, X_2^2)$, which is given by the following lower block triangular matrix of the form

$$J = \begin{bmatrix} J_1 & 0 \\ J_2 & J_3 \end{bmatrix}; \quad J_1 = \begin{bmatrix} a_{11} & 0 \\ a_{21} & a_{22} \end{bmatrix}, \quad J_2 = \begin{bmatrix} a_{31} & 0 \\ 0 & a_{42} \end{bmatrix}, \quad J_3 = \begin{bmatrix} a_{33} & 0 \\ a_{43} & a_{44} \end{bmatrix}$$

where

$$\begin{aligned} a_{11} &= \mu_1 (S_1^{in} - k_1 X_1^1) - D_1 - k_1 \mu_1' (S_1^{in} - k_1 X_1^1) X_1^1, & a_{21} &= k_2 \mu_2' (S_2^{in} + k_2 X_1^1 - k_3 X_2^1) X_2^1, \\ a_{22} &= \mu_2 (S_2^{in} + k_2 X_1^1 - k_3 X_2^1) - D_1 - k_3 \mu_2' (S_2^{in} + k_2 X_1^1 - k_3 X_2^1) X_2^1, & a_{31} &= D_2, \\ a_{33} &= \mu_1 (S_1^{in} - k_1 X_1^2) - D_2 - k_1 \mu_1' (S_1^{in} - k_1 X_1^2) X_1^2, & a_{43} &= k_2 \mu_2' (S_2^{in} + k_2 X_1^2 - k_3 X_2^2) X_2^2, \\ a_{44} &= \mu_2 (S_2^{in} + k_2 X_1^2 - k_3 X_2^2) - D_2 - k_3 \mu_2' (S_2^{in} + k_2 X_1^2 - k_3 X_2^2) X_2^2, & a_{42} &= D_2. \end{aligned}$$

Note that, J_1 is the Jacobian matrix of the upper two-dimensional subsystem of (3.2) evaluated at (X_1^1, X_2^1) , and J_3 is the Jacobian matrix of the lower two-dimensional subsystem of (3.2) evaluated at (X_1^2, X_2^2) . Thus, the stability of the steady state is determined by the sign

of the real parts of the eigenvalues of J_1 and J_3 . A steady state is LES if the real parts of the eigenvalues of J_1 and J_3 at this steady state are negative. Since they are lower triangular matrices, a steady state is LES if the corresponding eigenvalues a_{ii} , $i = 1, \dots, 4$.

To simplify the presentation of the proof, we first determine the stability conditions of the steady states of the upper two-dimensional subsystem of (3.2) which corresponds to the AM2 model. Then, we will establish the stability conditions of the steady states of the lower two-dimensional subsystem of (3.2). Finally, the stability of the complete system (3.2) follows by combining all conditions.

Table 10

The stability conditions of all steady states of the upper two-dimensional subsystem of (3.2), where the existence condition are defined in Table 8 and the functions λ_1^1 and λ_2^{1i} are defined in Table 1.

	Stability conditions
E_{00}	$S_1^{in} < \lambda_1^1$ and $S_2^{in} \notin [\lambda_2^{11}, \lambda_2^{12}]$
E_{10}	$S_2^{in} + \frac{k_2}{k_1}(S_1^{in} - \lambda_1^1) \notin [\lambda_2^{11}, \lambda_2^{12}]$
E_{01}	$S_1^{in} < \lambda_1^1$
E_{02}	Always unstable
E_{11}	LES when it exists
E_{12}	Always unstable

- For $E_{00} = (0, 0)$, the two eigenvalues of J_1 are

$$a_{11} = \mu_1(S_1^{in}) - D_1 \quad \text{and} \quad a_{22} = \mu_2(S_2^{in}) - D_1.$$

From Hypotheses 2.1 and 2.2 and the expressions of λ_1^1 , λ_2^{11} and λ_2^{12} in Table 1, E_{00} is LES if and only if a_{11} and a_{22} are negative, that is, the stability conditions of E_{00} in Table 10 hold.

- For $E_{10} = (X_1^{1*}, 0)$, where $X_1^{1*} = (S_1^{in} - \lambda_1^1)/k_1$, the two eigenvalues of J_1 are

$$a_{11} = -k_1\mu_1'(\lambda_1^1)X_1^{1*} \quad \text{and} \quad a_{22} = \mu_2\left(S_2^{in} + \frac{k_2}{k_1}(S_1^{in} - \lambda_1^1)\right) - D_1.$$

From Hypothesis 2.1, a_{11} is negative. From Hypothesis 2.2, a_{22} is negative if and only if the stability condition of E_{10} in Table 10 holds.

- For $E_{0i} = (0, X_2^{1i*})$, $i = 1, 2$, where $X_2^{1i*} = (S_2^{in} - \lambda_2^{1i})/k_3$, the two eigenvalues of J_1 are

$$a_{11} = \mu_1(S_1^{in}) - D_1 \quad \text{and} \quad a_{22} = -k_3\mu_2'(\lambda_2^{1i})X_2^{1i*}.$$

Using Hypothesis 2.2, E_{02} is unstable when it exists since a_{22} is positive. However, E_{01} is LES if and only if $S_1^{in} < \lambda_1^1$ since a_{22} is negative.

- For $E_{1i} = (X_1^{1*}, X_2^{1i*})$, $i = 1, 2$, where $X_1^{1*} = (S_1^{in} - \lambda_1^1)/k_1$ and $X_2^{1i*} = (S_2^{in} - \lambda_2^{1i})/k_3$, the two eigenvalues of J_1 are

$$a_{11} = -k_1\mu_1'(\lambda_1^1)X_1^{1*} \quad \text{and} \quad a_{22} = -k_3\mu_2'(\lambda_2^{1i})X_2^{1i*}.$$

From Hypothesis 2.2, E_{12} is unstable when it exists since a_{22} is positive. However, E_{11} is LES when it exists since a_{11} and a_{22} are negative.

Let us now consider the lower two-dimensional system of (3.2). From Table 10, it follows that the steady states E_{02}^{01} , E_{02}^{11} and E_{12}^{11} are unstable.

- For $E_{00}^{00} = (0, 0)$, the two eigenvalues of J_3 are

$$a_{33} = \mu_1(S_1^{in}) - D_2 \quad \text{and} \quad a_{44} = \mu_2(S_2^{in}) - D_2,$$

which are negative if and only if the two stability conditions in Table 11 hold.

Table 11

The stability conditions of all steady states of the lower two-dimensional system of (3.2). The functions f_1 , f_3 , g_1 and g_2 are defined in Table 2 while X_1^{2*} is a unique solution of equation $f_1(x) = g_1(x)$ and X_2^{2*} is a solution of equation $f_3(x) = g_2(x)$.

Stability conditions	
E_{00}^{00}	$S_1^{in} < \lambda_1^2$ and $S_2^{in} \notin [\lambda_2^{21}, \lambda_2^{22}]$
E_{00}^{01}	$S_1^{in} < \lambda_1^2$
E_{00}^{02}	Always unstable
E_{00}^{10}	$S_2^{in} + \frac{k_2}{k_1} (S_1^{in} - \lambda_1^2) \notin [\lambda_2^{21}, \lambda_2^{22}]$
E_{00}^{11}	LES when it exists
E_{00}^{12}	Always unstable
E_{10}^{10}	$S_2^{in} + k_2 X_1^{2*} \notin [\lambda_2^{21}, \lambda_2^{22}]$
E_{10}^{11}	LES when it exists
E_{10}^{12}	Always unstable
E_{01}^{01}	$S_1^{in} < \lambda_1^2$
E_{01}^{11}	$g_2'(X_2^{2*}) > f_3'(X_2^{2*})$
E_{11}^{11}	$g_2'(X_2^{2*}) > f_3'(X_2^{2*})$

- For $E_{00}^{0i} = (0, X_2^{2i*})$, $i = 1, 2$, where $X_2^{2i*} = (S_2^{in} - \lambda_2^{2i}) / k_3$, the eigenvalues of J_3 are written as follows:

$$a_{33} = \mu_1 (S_1^{in}) - D_2 \quad \text{and} \quad a_{44} = -k_3 \mu_2' (\lambda_2^{2i}) X_2^{2i*}.$$

From Hypothesis 2.2, E_{00}^{02} is unstable when it exists since a_{44} is positive. However, from Hypothesis 2.1, E_{00}^{01} is LES if and only if $S_1^{in} < \lambda_1^2$, since a_{44} is negative.

- For $E_{00}^{10} = (X_1^{2*}, 0)$, where $X_1^{2*} = (S_1^{in} - \lambda_1^2) / k_1$, the eigenvalues of J_3 are

$$a_{33} = -k_1 \mu_1' (\lambda_1^2) X_1^{2*} \quad \text{and} \quad a_{44} = \mu_2 \left(S_2^{in} + \frac{k_2}{k_1} (S_1^{in} - \lambda_1^2) \right) - D_2.$$

From Hypothesis 2.1, a_{33} is negative. From Hypothesis 2.2, it follows that E_{00}^{10} is LES if and only if the stability condition in Table 11 holds.

- For $E_{00}^{1i} = (X_1^{2*}, X_2^{2i*})$, where $X_1^{2*} = \frac{S_1^{in} - \lambda_1^2}{k_1}$ and $X_2^{2i*} = \frac{1}{k_3} \left(S_2^{in} + \frac{k_2}{k_1} (S_1^{in} - \lambda_1^2) - \lambda_2^{2i} \right)$, the eigenvalues of J_3 are

$$a_{33} = -k_1 \mu_1' (\lambda_1^2) X_1^{2*} \quad \text{and} \quad a_{44} = -k_3 \mu_2' (\lambda_2^{2i}) X_2^{2i*}, \quad i = 1, 2.$$

From Hypothesis 2.1, a_{33} is negative. From Hypothesis 2.2 and the expressions of X_2^{2j*} , the steady state E_{00}^{12} is unstable when it exists since a_{44} is positive. However, E_{00}^{11} is LES since a_{44} is negative.

- For $E_{10}^{1i} = (X_1^{2*}, 0)$, where X_1^{2*} is the unique solution of equation $f_1(X_1^2) = g_1(X_1^2)$, the eigenvalues of J_3 are

$$a_{33} = -D_2 \frac{X_1^{1*}}{X_1^{2*}} - k_1 \mu_1' (S_1^{in} - k_1 X_1^{2*}) X_1^{2*} \quad \text{and} \quad a_{44} = \mu_2 (S_2^{in} + k_2 X_1^{2*}) - D_2.$$

Using the definitions of f_1 and g_1 in Table 2, a straightforward calculation shows that

$$a_{33} = -[g_1'(X_1^{2*}) - f_1'(X_1^{2*})] X_1^{2*}.$$

Recall, from the proof of Lemma A.1, that the function $x \mapsto g_1(x) - f_1(x)$ is increasing. Hence, a_{33} is negative. Using Hypothesis 2.2, E_{10}^{10} is LES if and only if a_{44} is negative, that is, the stability condition in Table 11 holds.

- For $E_{10}^{1i} = (X_1^{2*}, X_2^{2i*})$, $i = 1, 2$, where X_1^{2*} is the unique solution of equation $f_1(x) = g_1(x)$ and $X_2^{2i*} = \frac{1}{k_3} (S_2^{in} + k_2 X_1^{2*} - \lambda_2^{2i})$, the eigenvalues of J_3 are

$$a_{33} = -[g'_1(X_1^{2*}) - f'_1(X_1^{2*})] X_1^{2*} \quad \text{and} \quad a_{44} = -k_3 \mu'_2(\lambda_2^{2i}) X_2^{2i*}.$$

Similarly to the steady state E_{10}^{10} , the term a_{33} is negative. Thus, E_{10}^{12} is unstable when it exists since a_{44} is positive, while E_{10}^{11} is LES when it exists since a_{44} is negative.

- For $E_{01}^{01} = (0, X_2^{2*})$, where X_2^{2*} is the unique solution of equation $f_2(X_2^2) = g_2(X_2^2)$ (see [Proposition 3.2](#)), the eigenvalues of J_3 are given by

$$a_{33} = \mu_1(S_1^{in}) - D_2 \quad \text{and} \quad a_{44} = -D_2 \frac{X_2^{1*}}{X_2^{2*}} - k_3 \mu'_2(S_2^{in} - k_3 X_2^{2*}) X_2^{2*},$$

where $X_2^{1*} = (S_2^{in} - \lambda_2^{11})/k_3$. From [Hypothesis 2.1](#), a_{33} is negative if and only if $S_1^{in} < \lambda_1^2$. Using the definitions of f_2 and g_2 in [Table 2](#), we can easily calculate

$$a_{44} = -[g'_2(X_2^{2*}) - f'_2(X_2^{2*})] X_2^{2*}.$$

Recall that $X_2^{1*} > x_1^m := (S_2^{in} - S_2^m)/k_3$ so that the function $x \mapsto g_2(x) - f_2(x)$ is increasing (see the proof of [Lemma A.2](#)). Hence, a_{44} is negative. Therefore, the stability condition of E_{01}^{01} in [Table 11](#) hold.

- For $E_{01}^{11} = (X_1^{2*}, X_2^{2*})$, where $X_1^{2*} = \frac{1}{k_1} (S_1^{in} - \lambda_1^2)$ and X_2^{2*} is a solution of $f_3(x) = g_2(x)$, the eigenvalues of J_3 are given by

$$a_{33} = -k_1 \mu'_1(\lambda_1^2) X_1^{2*} \quad \text{and} \quad a_{44} = -[g'_2(X_2^{2*}) - f'_3(X_2^{2*})] X_2^{2*},$$

From [Hypothesis 2.1](#), a_{33} is negative. Consequently, E_{10}^{11} is LES if and only if a_{44} is negative, that is, the stability condition in [Table 11](#) holds.

- For $E_{11}^{11} = (X_1^{2*}, X_2^{2*})$, where X_1^{2*} is a solution of equation $f_1(x) = g_1(x)$ and X_2^{2*} is a solution of equation $f_3(x) = g_2(x)$, the eigenvalues of J_3 are given by

$$a_{33} = -[g'_1(X_1^{2*}) - f'_1(X_1^{2*})] X_1^{2*} \quad \text{and} \quad a_{44} = -[g'_2(X_2^{2*}) - f'_3(X_2^{2*})] X_2^{2*},$$

Similarly to E_{10}^{10} , a_{33} is negative. As for E_{01}^{11} , E_{11}^{11} is LES if and only if a_{44} is negative, that is, the stability condition in [Table 11](#) holds. ■

Proof of Proposition 4.3. The function $D \mapsto \lambda_1^1(D)$ is defined, positive and increasing on the interval $[0, rm_1)$. It tends to infinity as D tends to rm_1 . From [Table 6](#), it follows that γ_0 and γ_6 intersect if $rm_1 > D_1^*$, that is, $m_1 > \mu_2(S_2^{in})$. In this case, we have $D = D_1^* = r\mu_2(S_2^{in})$ and $S_1^{in} = \lambda_1^1(D_1^*, r)$, that is, $\gamma_0 \cap \gamma_6 = P_1$. Since $D_1^* < \min(D_1^m, rm_1)$, then the functions F_{11} and F_{12} are defined in D_1^* . At this values, we have $\mu_1(S_1^{in}) = \mu_2(S_2^{in}) = D_1$. If $S_2^{in} < S_2^m$, we obtain $S_2^{in} = \lambda_2^{11}$; otherwise $S_2^{in} = \lambda_2^{12}$. From the definition of the functions F_{11} and F_{12} in [Table 1](#), it follows that $S_1^{in} = \lambda_1^1$ in these two cases. Consequently, $\gamma_0 \cap \gamma_6 \cap \gamma_4 = P_1$ if $S_2^{in} < S_2^m$ and $\gamma_0 \cap \gamma_6 \cap \gamma_5 = P_1$, otherwise. Similar arguments apply to the second part of the proposition. ■

Proof of Proposition 4.4. Under [Lemma 4.2](#), we have for all $r \in (0, 1/2)$

$$\lambda_1^2(D, r) < \lambda_1^1(D, r) \quad \text{and} \quad \lambda_2^{21}(D, r) < \lambda_2^{11}(D, r).$$

From the definition of F_{11} and F_{21} in [Table 1](#), $F_{21}(D, r, S_2^{in}) < F_{11}(D, r, S_2^{in})$. Similarly, $F_{21}(D, r, S_2^{in}) > F_{11}(D, r, S_2^{in})$, for all $r \in (1/2, 1)$. ■

Let ϕ_i , $i = 1, 2$ be the function defined in [Table 1](#). To describe the existence condition $\phi_i > 0$ of the steady state \mathcal{E}_{10}^{1i} in [Table 4](#) and the stability condition $\phi_1 < 0$ or $\phi_2 > 0$ of the steady state \mathcal{E}_{10}^{10} in [Proposition 3.3](#), we need the following lemma showing the positivity of ϕ_i according to the values of S_2^{in} and D .

Lemma A.4. Let $D \in [0, \min(rm_1, (1-r)\mu_2(S_2^m))]$ and $\phi_j(D)$ be the function defined in Table 1. For all $S_2^{in} > S_2^m$, we have $\phi_1(D) > 0$. In addition, when $D > D_2^* = (1-r)\mu_2(S_2^{in})$, then $\phi_2(D) > 0$.

Proof of Lemma A.4. For all $S_2^{in} > S_2^m$, we have $S_2^{in} > \lambda_2^{21}(D, r)$, so that $\phi_1(D) > 0$ holds. In addition, from the definition of D_2^* in Table 6, we have $\lambda_2^{22}(D, r) < \lambda_2^{22}(D_2^*, r) = S_2^{in}$ for all $D > D_2^*$, so that $\phi_2(D) > 0$ holds. ■

In the next remark, we show that the existence condition of \mathcal{E}_{10}^{1i} and the stability condition of \mathcal{E}_{10}^{10} are not always satisfied where the function $\phi_i(D)$ can change their sign as we will see in Figure 9.

Remark A.5. For the set of parameters in Table 12, the condition $\phi_2(D) > 0$ is not always verified when $D < D_2^*$ (see Figure 9(a)). For the set of parameters in Figure 4 where $S_2^{in} < S_2^m$, condition $\phi_1(D) > 0$ holds (see Figure 9(b)) and the condition $\phi_2(D) > 0$ is not always verified (see Figure 9(c)).

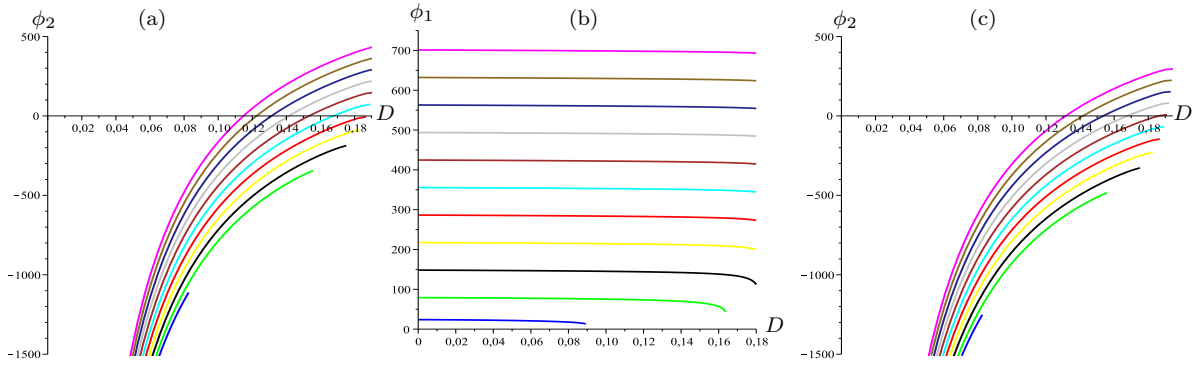


Figure 9. Curves of the functions $\phi_1(D)$ and $\phi_2(D)$, for several fixed values of $S_1^{in} = 5, 25, 50, 75, 100, 125, 150, 175, 200, 225, 250$ and $S_2^m \approx 48.74$: (a) $\phi_2(D)$ when $S_2^{in} = 150 > S_2^m$ (b) $\phi_1(D)$ when $S_2^{in} = 10 < S_2^m$; (c) $\phi_2(D)$ when $S_2^{in} = 10 < S_2^m$.

Proof of Proposition 4.5. We determine the operating diagram of Figure 2 in the case $r \in (0, 1/2)$, $S_2^{in} > S_2^m$, and $m_1 > \mu_2(S_2^m)$. However, the cases in items (2) and (3) can be treated similarly and are left to the reader using Figures 10 and 11, respectively. In addition, the only difference between items (4) and (1) is the stability of the steady states \mathcal{E}_{00}^{00} , \mathcal{E}_{00}^{01} , and \mathcal{E}_{01}^{01} , where the minimum of the break-even concentrations λ_1^i and λ_2^{ij} is given by

$$\min(\lambda_1^1, \lambda_1^2) = \lambda_1^1, \quad \min(\lambda_2^{11}, \lambda_2^{21}) = \lambda_2^{11} \quad \text{and} \quad \max(\lambda_2^{12}, \lambda_2^{22}) = \lambda_2^{12},$$

using Lemma 4.2 for $r > 1/2$. Inversely, in item (1) for $r < 1/2$, we have

$$(A.14) \quad \min(\lambda_1^1, \lambda_1^2) = \lambda_1^2, \quad \min(\lambda_2^{11}, \lambda_2^{21}) = \lambda_2^{21} \quad \text{and} \quad \max(\lambda_2^{12}, \lambda_2^{22}) = \lambda_2^{22}.$$

From Proposition 3.3, the six steady states \mathcal{E}_{00}^{02} , \mathcal{E}_{00}^{12} , \mathcal{E}_{10}^{12} , \mathcal{E}_{02}^{01} , \mathcal{E}_{02}^{11} and \mathcal{E}_{12}^{11} are unstable, when they exist. Next, we establish the existence and stability of each steady state in the various regions of the operating diagram in the case of item (1).

- \mathcal{E}_{00}^{00} always exists. From Table 5 and (A.14), it is LES if and only if,

$$S_1^{in} < \lambda_1^2 \quad \text{and} \quad (S_2^{in} < \lambda_2^{21} \quad \text{or} \quad S_2^{in} > \lambda_2^{22}).$$

From Table 6, the first stability condition of \mathcal{E}_{00}^{00} holds, for all (D, S_1^{in}) in the region bounded by the curve γ_1 and located below this curve. The second stability condition is equivalent to $D_2^* := (1-r)\mu_2(S_2^{in}) < D$, that is, this condition holds in the regions at the right of the vertical line γ_8 . Using the definition of regions in Table 13, \mathcal{E}_{00}^{00} is LES in \mathcal{J}_0 and \mathcal{J}_3 (see Figure 2). Hence, we obtain the first column in Table 7 corresponding to \mathcal{E}_{00}^{00} .

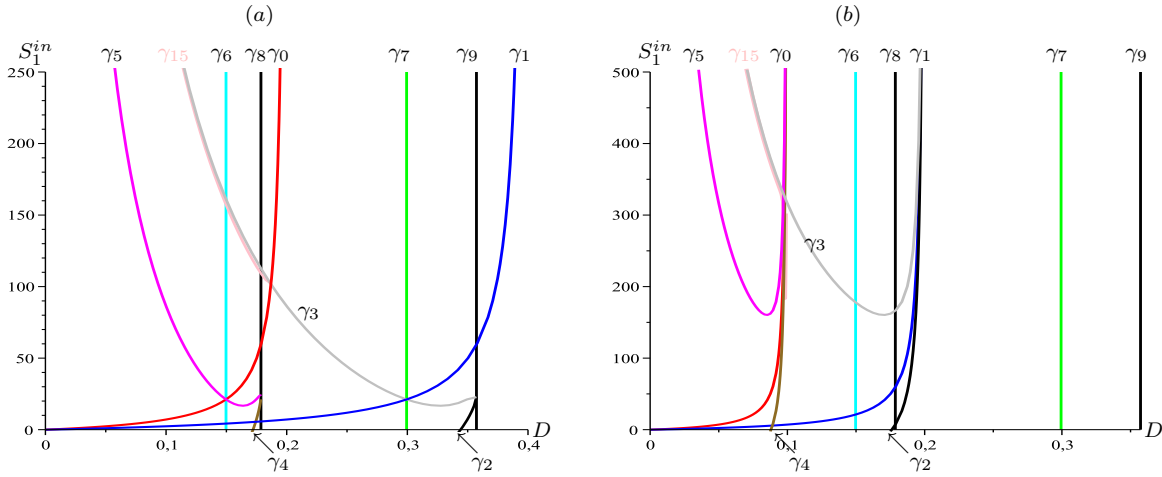


Figure 10. The curves $\gamma_i, i = 1 - 9$ and γ_{15} , when $r = 1/3 \in (0, 1/2)$, $S_2^{in} = 150 > S_2^m \approx 48.740$: (a) $m_1 = 0.6 > \mu_2(S_2^m) \approx 0.535$; (b) $m_1 = 0.3 < \mu_2(S_2^m) \approx 0.535$.

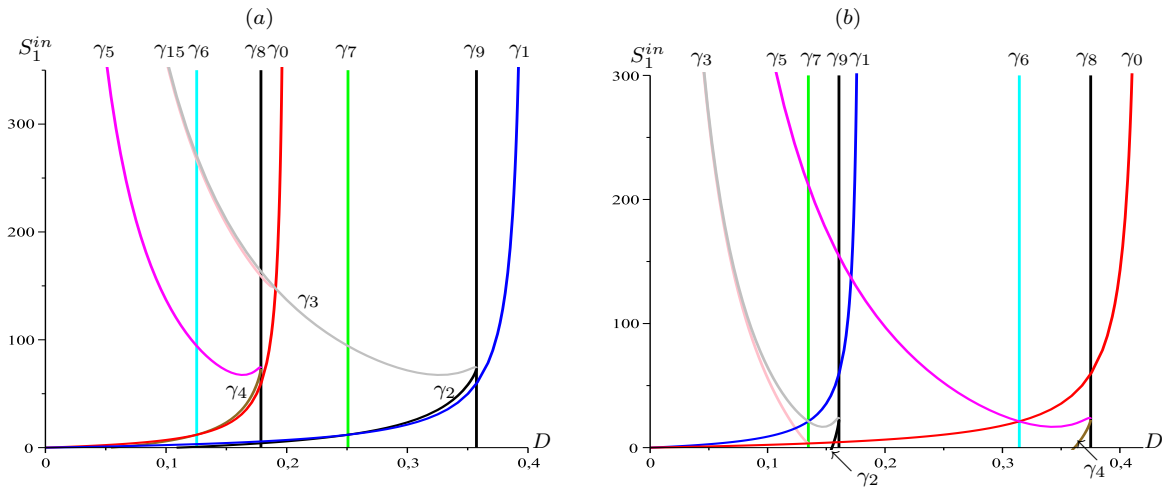


Figure 11. The curves $\gamma_i, i = 1 - 9$ and γ_{15} : (a) case when $r = 1/3 \in (0, 1/2)$, $S_2^{in} = 10 < S_2^m \approx 48.740$ and $m_1 = 0.6 > \mu_2(S_2^m) \approx 0.535$; (b) case when $r = 0.7 \in (0, 1/2)$, $S_2^{in} = 150 > S_2^m \approx 48.740$ and $m_1 = 0.6 > \mu_2(S_2^m) \approx 0.535$.

- For \mathcal{E}_{00}^{01} , the existence condition is given in Table 4 by $S_2^{in} > \lambda_2^{21}$. Since $S_2^{in} > S_2^m$, then $S_2^{in} > \lambda_2^{21}$ for all $D < D_2^m = (1 - r)\mu_2(S_2^m)$, that is, for all (D, S_1^{in}) in the regions at the right of the vertical line γ_9 and located at the left of this line. Using Table 13, \mathcal{E}_{00}^{01} exists in \mathcal{J}_i , $i = 2 - 20$ (see Figure 2). From Table 5 and (A.14), \mathcal{E}_{00}^{01} is LES if and only if,

$$S_1^{in} < \lambda_1^2 \quad \text{and} \quad (S_2^{in} < \lambda_2^{11} \quad \text{or} \quad S_2^{in} > \lambda_2^{12}).$$

Thus, the first stability condition holds in the region below the curve γ_1 . The second stability condition is equivalent to $D_1^* := r\mu_2(S_2^{in}) < D$, that is, this condition holds in the regions at the right of the vertical line γ_6 . Using Table 13, \mathcal{E}_{00}^{01} is LES in $\mathcal{J}_3, \mathcal{J}_4$ and \mathcal{J}_{14} (see Figure 2). Consequently, we obtain the second column in Table 7 corresponding to \mathcal{E}_{00}^{01} .

- \mathcal{E}_{00}^{02} exists if and only if $S_2^{in} > \lambda_2^{22}$, that is, for all $D_2^* < D < D_2^m$. Thus, the existence condition of \mathcal{E}_{00}^{02} holds in the regions at the left of the vertical line γ_9 and the right of the vertical line γ_8 . Using Table 13, \mathcal{E}_{00}^{02} exists in \mathcal{J}_2 and \mathcal{J}_3 .
- \mathcal{E}_{00}^{10} exists in the regions above the curve γ_1 (see Figure 2) as the existence condition is $S_1^{in} > \lambda_1^2$. Using the definition of regions in Table 13, \mathcal{E}_{00}^{10} exists in $\mathcal{J}_i, i = 1, 2, 5 - 13, 16 - 20$. From Table 5, the inequalities (A.14) and the functions F_{21} and F_{21} defined in Table 1, the stability

conditions of \mathcal{E}_{00}^{10} become

$$S_1^{in} < \lambda_1^1 \quad \text{and} \quad (S_2^{in} < \lambda_2^{11} \quad \text{or} \quad S_2^{in} > \lambda_2^{12}) \quad \text{and} \quad (S_1^{in} < F_{21} \quad \text{or} \quad S_1^{in} > F_{22}).$$

Thus, the first stability condition of \mathcal{E}_{00}^{10} holds in the regions below the curve γ_0 . Similarly to \mathcal{E}_{00}^{01} , the second stability condition holds in the regions at the right of the vertical line γ_6 . The third stability condition can be written as

$$\mu_2 \left(S_2^{in} + \frac{k_2}{k_1} (S_1^{in} - \lambda_1^2) \right) < \frac{D}{1-r}$$

or equivalently

$$D > D_2^m := (1-r)\mu_2(S_2^m) \quad \text{or} \quad S_2^{in} + \frac{k_2}{k_1} (S_1^{in} - \lambda_1^2) > \lambda_2^{22} \quad (\text{or also } S_1^{in} > F_{22})$$

since $S_2^{in} > S_2^m$. Therefore, the third stability condition holds in the region at the right of the vertical line γ_9 or above the curve γ_3 (see Figure 2). From Table 13, it follows that \mathcal{E}_{00}^{10} is LES in $\mathcal{J}_i, i = 1, 2, 8$.

- For $\mathcal{E}_{00}^{1i}, i = 1, 2$, the existence conditions become

$$S_1^{in} > \max(\lambda_1^2, F_{2i}),$$

where F_{2i} is defined for all $D < D_2^m := (1-r)\mu_2(S_2^m)$ (see Table 1), that is, this condition holds for all (D, S_1^{in}) in the regions at the left of the vertical line γ_9 . From Proposition 4.3, we have $F_{21} < \lambda_1^2$ and $\lambda_1^2 < F_{22}$, for all $D < D_2^*$ and inversely $\lambda_1^2 > F_{22}$, for all $D > D_2^*$. Hence, \mathcal{E}_{00}^{11} exists in the regions above the curve γ_1 and at the left of the vertical line γ_9 . However, \mathcal{E}_{00}^{12} exists either in the regions above the curve γ_3 when (D, S_1^{in}) is on the left of the vertical line γ_8 either in the regions above the curve γ_1 when (D, S_1^{in}) is on the right of the vertical line γ_8 and the left of the vertical line γ_9 (see Figure 2). From Table 13, \mathcal{E}_{00}^{12} exists in $\mathcal{J}_i, i = 2, 8 - 10, 20$ while \mathcal{E}_{00}^{11} exists in $\mathcal{J}_i, i = 2, 5 - 13, 16 - 20$. The stability conditions of \mathcal{E}_{00}^{11} are given by

$$S_1^{in} < \lambda_1^1 \quad \text{and} \quad (S_2^{in} < \lambda_2^{11} \quad \text{or} \quad S_2^{in} > \lambda_2^{12}).$$

Thus, the first stability condition of \mathcal{E}_{00}^{10} holds in the regions below the curve γ_0 . Similarly to \mathcal{E}_{00}^{01} , the second stability condition of \mathcal{E}_{00}^{11} holds in the regions at the right of the vertical line γ_6 . From Table 13, \mathcal{E}_{00}^{11} is LES in $\mathcal{J}_i, i = 2, 5, 8, 13$.

- For \mathcal{E}_{10}^{10} , the existence conditions become $S_1^{in} > \lambda_1^1$. Thus, \mathcal{E}_{10}^{10} exists in the regions above the curve γ_0 (see Figure 2). Using the definition of regions in Table 13, \mathcal{E}_{10}^{10} exists in $\mathcal{J}_i, i = 6, 7, 9 - 12, 17 - 20$. The stability conditions of \mathcal{E}_{10}^{10} become

$$[D_1 > \mu_2(S_2^m) \quad \text{or} \quad (D_1 < \mu_2(S_2^m) \quad \text{and} \quad (S_1^{in} < F_{11} \quad \text{or} \quad S_1^{in} > F_{12}))] \quad \text{and} \quad [\phi_1 < 0 \quad \text{or} \quad \phi_2 > 0].$$

From Proposition 4.3, we have $\lambda_1^1 > F_{11}$ so that the condition $S_1^{in} < F_{11}$ does not hold since the existence condition of \mathcal{E}_{10}^{10} is $S_1^{in} > \lambda_1^1$. Hence, the first stability condition of \mathcal{E}_{10}^{10} holds in the regions at the right of the vertical line γ_8 or on the left of γ_8 and above the maximum of the two curves γ_0 and γ_5 (see Figure 10(a)). According to Lemma A.4, condition $\phi_1 < 0$ is not satisfied. Figure 9(a) shows that the condition $\phi_2(D) > 0$ holds in the right of the root of equation $\phi_2(D) = 0$ for several values of S_1^{in} . Hence, the second stability condition of \mathcal{E}_{10}^{10} holds in the regions at the right of the curve γ_{15} . From Table 13, \mathcal{E}_{10}^{10} is LES in $\mathcal{J}_i, i = 7, 9, 10, 11, 19, 20$.

- For $\mathcal{E}_{10}^{1i}, i = 1, 2$, the existence conditions become

$$S_1^{in} > \lambda_1^1 \quad \text{and} \quad \phi_i > 0.$$

From Lemma A.4, condition $\phi_1 > 0$ is always verified. Thus, \mathcal{E}_{10}^{11} exists in the regions above the curve γ_0 while \mathcal{E}_{10}^{12} exists in the regions on the left of the curve γ_0 and the right of the curve γ_{15} . From Table 13, \mathcal{E}_{10}^{11} exists in $\mathcal{J}_i, i = 6, 7, 9 - 12, 17 - 20$ while \mathcal{E}_{10}^{12} exists in $\mathcal{J}_i, i = 7, 9, 11, 19, 20$. The stability condition of \mathcal{E}_{10}^{11} becomes

$$S_1^{in} < F_{11} \quad \text{or} \quad S_1^{in} > F_{12}.$$

Similarly to \mathcal{E}_{10}^{10} , the stability conditions of \mathcal{E}_{10}^{11} holds in the regions at the right of the vertical line γ_8 or on the left of γ_8 and above the maximum of the two curves γ_0 and γ_5 . From Table 13, \mathcal{E}_{10}^{11} is LES in $\mathcal{J}_i, i = 6, 7, 9 - 12, 18, 19, 20$.

- For $\mathcal{E}_{0i}^{01}, i = 1, 2$, the existence conditions become $S_2^{in} > \lambda_2^{1i}$. Since $S_2^{in} > S_2^m$, then the condition $S_2^{in} > \lambda_2^{21}$ holds for all $D < D_1^m$. Thus, the existence condition of \mathcal{E}_{01}^{01} holds in the regions at the left of the vertical line γ_8 . However, the existence condition of \mathcal{E}_{02}^{01} holds in the regions on the left of the curve γ_8 and the right of the curve γ_6 . From Table 13, \mathcal{E}_{01}^{01} exists in $\mathcal{J}_i, i = 10 - 20$ while \mathcal{E}_{02}^{01} exists in $\mathcal{J}_i, i = 10 - 14$. The stability condition of \mathcal{E}_{01}^{01} becomes $S_1^{in} < \lambda_1^2$, that is, this condition holds in the regions below the curve γ_1 . From Table 13, it follows that \mathcal{E}_{01}^{01} is LES in \mathcal{J}_{14} and \mathcal{J}_{15} .
- For $\mathcal{E}_{0i}^{11}, i = 1, 2$, the existence conditions become

$$S_2^{in} > \lambda_2^{1i} \quad \text{and} \quad S_1^{in} > \lambda_1^2.$$

The second existence condition of \mathcal{E}_{0i}^{11} holds in the regions above the curve γ_1 . Since $S_2^{in} > S_2^m > \lambda_2^{11}$ for all $D < D_1^m$, the first existence condition of \mathcal{E}_{01}^{11} holds in the regions at the left of the vertical line γ_8 . The first existence condition of \mathcal{E}_{02}^{11} holds in the regions on the left of the curve γ_8 and the right of the curve γ_6 . From Table 13, it follows that \mathcal{E}_{01}^{11} exists in $\mathcal{J}_i, i = 10 - 13, 16 - 20$ while \mathcal{E}_{02}^{11} exists in $\mathcal{J}_i, i = 10 - 13$. The stability conditions of \mathcal{E}_{01}^{11} is given by

$$S_1^{in} < \lambda_1^1 \quad \text{and} \quad g_2'(X_2^{2*}) > f_3'(X_2^{2*})$$

The first stability condition holds in the region below the curve γ_0 . For the set of parameters in Table 12 corresponding to the operating diagram in Figure 2, the equation $\phi_3(x) := f_3(x) - g_2(x) = 0$ has unique solution, that is, $g_2'(X_2^{2*}) > f_3'(X_2^{2*})$ holds. Since the operating parameters D and S_1^{in} are variable, the numerical simulations show the uniqueness of the solution of equation $\phi_3(x) = 0$ for several values of D and S_1^{in} as shown in Figure 12. From Table 13, it follows that \mathcal{E}_{01}^{11} is LES in \mathcal{J}_{13} and \mathcal{J}_{16} .

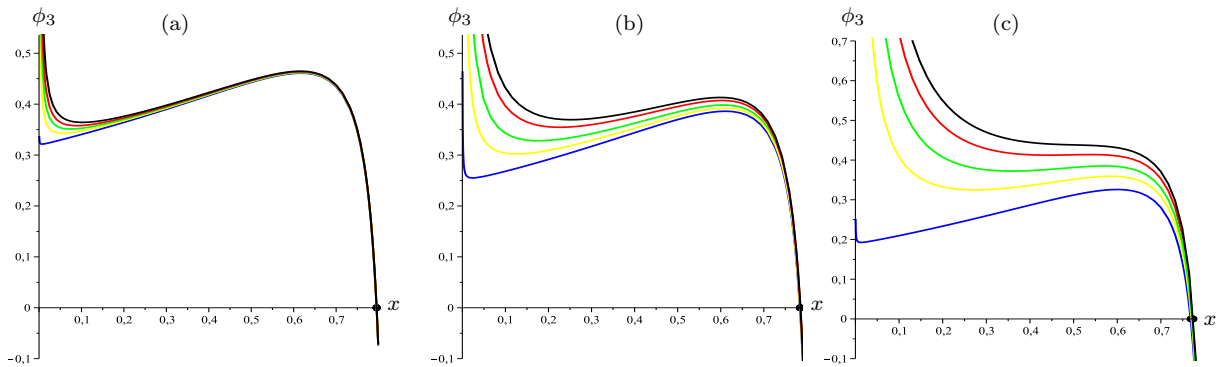


Figure 12. Number of positive solutions of equation $\phi_3(x) = 0$ corresponding to the steady state \mathcal{E}_{01}^{11} , when $S_2^{in} = 150 > S_2^m \approx 48.740$, and for various values of $D < D_1^* \approx 0.149$ and $S_1^{in} \in [\lambda_1^2, \lambda_1^1]$: (a) $D = 0.05$ and $S_1^{in} \in \{1.02, 1.4, 1.7, 2, 2.35\}$ where $\lambda_1^2 = 1.014$ and $\lambda_1^1 = 2.366$; (b) $D = 0.1$ and $S_1^{in} \in \{2.4, 3.4, 4.5, 6, 7\}$ where $\lambda_1^2 = 2.366$ and $\lambda_1^1 = 7.10$; (c) $D = 0.14$ and $S_1^{in} \in \{3.83, 7.8, 10.8, 14, 16.5\}$ where $\lambda_1^2 = 3.82$ and $\lambda_1^1 = 16.56$.

- For $\mathcal{E}_{1i}^{11}, i = 1, 2$, the existence conditions become

$$S_1^{in} > \max(\lambda_1^1, F_{1i}),$$

where F_{1i} is defined for all $D < \min(r_1 m_1, D_1^m) = D_1^m$ (see Table 1), that is, this last condition holds for all (D, S_1^{in}) in the regions at the left of the vertical line γ_8 . From Proposition 4.3, we have $\lambda_1^1 > F_{11}$ so that the existence condition of \mathcal{E}_{11}^{11} holds in the regions above the curve γ_0 . However, the existence condition of \mathcal{E}_{12}^{11} holds in the regions on the left of γ_8 and above the maximum of the two curves γ_0 and γ_5 (see Figure 10(a)). From Table 13, we see that \mathcal{E}_{11}^{11} exists in $\mathcal{J}_i, i = 10, 11, 12, 17 - 20$ while \mathcal{E}_{02}^{01} exists in $\mathcal{J}_i, i = 10 - 13$. Recall that the stability condition of \mathcal{E}_{11}^{11} is

$$g_2'(X_2^{2*}) > f_3'(X_2^{2*}).$$

Similarly to the steady state \mathcal{E}_{01}^{11} , the equation $\phi_3(x) := f_3(x) - g_2(x) = 0$ has unique solution (that is, $g_2'(X_2^{2*}) > f_3'(X_2^{2*})$) as we see in Figure 13 for the set of parameters in Table 12 corresponding to the operating diagram in Figure 2. Thus, \mathcal{E}_{11}^{11} is LES when it exists. ■

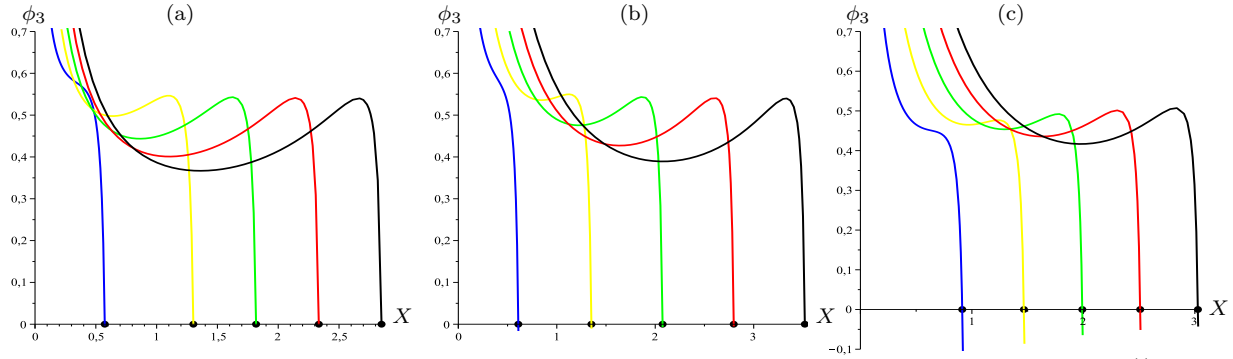


Figure 13. Number of positive solutions of equation $\phi_3(x) = 0$ corresponding to the steady state \mathcal{E}_{11}^{11} when $S_2^{in} = 150 > S_2^m \approx 48.740$, and for various values of $S_1^{in} > \lambda_1^1$ and $D \in \{0.05, 0.1, 0.17\}$: (a) $D = 0.05$ and $S_1^{in} \in \{2.37, 72, 122, 172, 222\}$ where $\lambda_1^1 \approx 2.366$; (b) $D = 0.1$ and $S_1^{in} \in \{7.2, 77, 147, 217, 287\}$ where $\lambda_1^1 \approx 7.1$; (c) $D = 0.17$ and $S_1^{in} \in \{40.24, 90, 140, 190, 240\}$ where $\lambda_1^1 \approx 40.233$.

Proof of Proposition 4.6. For D fixed in $(0, r\mu_2(S_2^m))$ and $r \in (0, 1)$, we have $S_{21}^{in*} = \lambda_2^{11}(D, r)$. Therefore,

$$\lambda_1^1(D, r) + \frac{k_1}{k_2} (\lambda_2^{11}(D, r) - S_{21}^{in*}) = \lambda_1^1(D, r).$$

Using Table 6, we see that the curves $\gamma_0, \gamma_4, \gamma_{10}$ intersect at the same point. In the same way, as $S_{23}^{in*} = \lambda_2^{12}(D, r)$. Therefore,

$$\lambda_1^1(D, r) + \frac{k_1}{k_2} (\lambda_2^{12}(D, r) - S_{23}^{in*}) = \lambda_1^1(D, r).$$

Consequently, the curves $\gamma_0, \gamma_5, \gamma_{12}$ intersect at the same point. For $S_2^{in} < S_{21}^{in*}$, we have $\lambda_2^{11}(D, r) < S_2^{in}$ and $\lambda_2^{12}(D, r) > S_2^{in}$. Then, the first item holds. Similarly, the result holds when $S_{21}^{in*} < S_2^{in} < S_{23}^{in*}$ and $S_2^{in} > S_{23}^{in*}$. ■

Using the definitions of the auxiliary functions in Table 6, we determine in the following proposition the relative positions of $\gamma_i, i = 6, 7$ and the curve γ_5 .

Lemma A.6. Fix $r \in (0, 1)$ and $D \in (0, (1 - r)\mu_2(S_2^m))$. Let $S_{2i}^{in*}, i = 1, \dots, 4$ be the critical values of S_2^{in} defined in Table 6. Let $\phi_j(D, r, S_1^{in}, S_2^{in}), j = 1, 2$ be the functions defined in Table 1. If $S_2^{in} > S_{22}^{in*}$, then $\phi_1 > 0$. In addition, if $S_2^{in} > S_{24}^{in*}$, then $\phi_2 > 0$.

Proof of Lemma A.6. From the expression of S_{22}^{in*} in Table 6, if $S_2^{in} > S_{22}^{in*}$, it follows that $S_2^{in} > \lambda_2^{21}(D, r)$ so that $\phi_1 > 0$ holds. For $S_2^{in} > S_{24}^{in*}$. Similarly, if $S_2^{in} > \lambda_2^{22}(D, r)$, then $\phi_2 > 0$ holds. ■

Proof of Proposition 4.7. Similarly to the proof of the operating diagram in Proposition 4.5 and using Proposition 4.6 and Lemma A.6, we obtain the result. ■

Appendix B. Tables. In this Appendix, we first provide in Table 12 all the values of the parameters used in the numerical simulations.

Table 12

Parameter values used for systems (2.3) and (3.2) when the growth rates μ_1 and μ_2 are given by (4.2).

Parameter	m_1 (d^{-1})	k_{S_1} (g/l)	m_2 (d^{-1})	k_{S_2} ($mmol/l$)	k_I ($mmol/l$)	k_1 ($mmol/g$)	k_2 ($mmol/g$)	k_3 ($mmol/g$)
Figures 2, 4 to 6, 7, and 8	0.6	7.1	0.74	9.28	256	42.14	116.5	268
Figure 3	0.3	7.1	0.74	9.28	256	42.14	116.5	268

Next, we first define in Table 13 the regions \mathcal{J}_i , $i = 0, \dots, 31$ of the operating diagram of Figures 2 to 4 in the two-dimensional plane (D, S_1^{in}) when r and S_2^{in} are fixed so that $r \in (0, 1/2)$. Then, we define in Table 14 the regions \mathcal{J}_i , $i = 32, \dots, 46$ of the operating diagram of Figure 5 in the two-dimensional plane (D, S_1^{in}) when r and S_2^{in} are fixed so that $r \in (1/2, 1)$. Then, we define in Table 15 the regions \mathcal{J}_i , $i = 46, \dots, 69$ of the operating diagram of Figure 6 in the two-dimensional plane (S_2^{in}, S_1^{in}) when r and D are fixed so that $r \in (0, 1/2)$ and $D \in (0, \mu_2(S_2^m))$.

REFERENCES

- [1] N. Abdellatif, R. Fekih-Salem and T. Sari, Competition for a single resource and coexistence of several species in the chemostat, *Math. Biosci. Eng.*, **13**, 631–652 (2016).
- [2] B. Bar and T. Sari, The operating diagram for a model of competition in a chemostat with an external lethal inhibitor, *Discrete and Continuous Dyn. Syst. - B*, **25**, 2093–2120 (2020).
- [3] D.J. Batstone, J. Keller, I. Angelidaki, S.V. Kalyuzhnyi, S.G. Pavlosthathis, A. Rozzi, W.T.M. Sanders, H. Siegrist and V.A. Vavilin, The IWA Anaerobic Digestion Model No 1 (ADM1), *Water Sci Technol.*, **45**, 66–73 (2002).
- [4] B. Benyahia and T. Sari, Effect of a new variable integration on steady states of a two-step anaerobic digestion model, *Math. Biosci. Eng.*, **17**, 5504–5533 (2020).
- [5] B. Benyahia, T. Sari, B. Cherki and J. Harmand, Bifurcation and stability analysis of a two step model for monitoring anaerobic digestion processes, *J. Proc. Control*, **22** 1008–1019 (2012).
- [6] O. Bernard, Z. Hadj-Sadok, D. Dochain, A. Genovesi and J-P. Steyer, Dynamical model development and parameter identification for an anaerobic wastewater treatment process, *Biotechnol. Bioeng.* **75**, 424–438 (2001).
- [7] A. Bornhöft, R. Hanke-Rauschenbach and K. Sundmacher, Steady-state analysis of the anaerobic digestion model no. 1 (ADM1), *Nonlinear Dyn.*, **73**, 535–549 (2013).
- [8] E. Chorukova, I. Simeonov and L. Kabaivanova, Volumes ratio optimization in a cascade anaerobic digestion system producing hydrogen and methane, *Ecol. Chem. Eng. S*, **28**, 183–200 (2021).
- [9] M. Dali-Youcef, J. Harmand, A. Rapaport and T. Sari, Some non-intuitive properties of serial chemostats with and without mortality, *IFAC-PapersOnLine* **55**, 475–480 (2022) .
- [10] M. Dali-Youcef, A. Rapaport and T. Sari, Study of performance criteria of serial configuration of two chemostats, *Math. Biosci. Eng.* **17**, 6278–6309 (2020) .
- [11] M. Dali-Youcef, A. Rapaport and T. Sari, Performance study of two serial interconnected chemostats with mortality, *Bull. Math. Biol.* **84**, 110 (2022).
- [12] M. Dali-Youcef and T. Sari, The productivity of two serial chemostats, *Int. J. Biomath.*, **16**, 2250113 (2023).
- [13] Y. Daoud, N. Abdellatif, T. Sari and J. Harmand, Steady state analysis of a syntrophic model: The effect of a new input substrate concentration, *Math. Model. Nat. Phenom.*, **13**, 1–22 (2018).
- [14] M. Dellal and B. Bar, Global analysis of a model of competition in the chemostat with internal inhibitor, *Discrete and Continuous Dyn. Syst. - B*, **26**, 1129–1148 (2021).
- [15] M. Dellal, B. Bar and M. Lakrib, A competition model in the chemostat with allelopathy and substrate inhibition, *Discrete and Continuous Dyn. Syst. - B*, **27**, 2025–2050 (2022).
- [16] M. Dellal, M. Lakrib and T. Sari, The operating diagram of a model of two competitors in a chemostat with an external inhibitor, *Math. Biosci.*, **302**, 27–45 (2018).
- [17] A. Dhooge, W. Govaerts, Yu. A. Kuznetsov, H. G. E. Meijer and B. Sautois, New features of the software MatCont for bifurcation analysis of dynamical systems, *Math. Comput. Model. Dyn.*, **14**, 147–175 (2008).

Table 13

Definitions of the regions \mathcal{J}_i , $i = 0, \dots, 31$ of the operating diagram of Figures 2 to 4 when $r \in (0, 1/2)$. For $i, j = 1, 2$, the functions D_i^m and D_i^* are defined in Table 6 while F_{ij} and ϕ_2 are defined in Table 1.

Condition on			
S_2^{in}	S_1^{in} and ϕ_2	D	Region
$[0, +\infty[$	(λ_1^1, F_{22}) and $\phi_2 < 0$	$(D_1^m, \min(r_1 m_1, D_2^m))$	\mathcal{J}_6
	(λ_1^1, F_{22}) and $\phi_2 > 0$	$(D_1^m, \min(r_1 m_1, D_2^m))$	\mathcal{J}_7
	(F_{22}, λ_1^1)	$(D_1^m, \min(r_2 m_1, D_2^*, D_2^m))$	\mathcal{J}_8
	$(\max(\lambda_1^1, F_{22}), +\infty)$	$(D_1^m, \min(r_1 m_1, r_2 m_1, D_2^m))$	\mathcal{J}_9
	$[0, \lambda_1^2]$	$(0, D_1^*)$	\mathcal{J}_{15}
	$(\lambda_1^2, \lambda_1^1)$	$(0, \min(r_2 m_1, D_1^*))$	\mathcal{J}_{16}
	$(\lambda_1^1, \min(F_{12}, F_{22}))$ and $\phi_2 < 0$	$(0, \min(r_1 m_1, D_1^*, D_2^m))$	\mathcal{J}_{17}
	(F_{12}, F_{22}) and $\phi_2 < 0$	$(0, \min(r_1 m_1, D_1^*, D_1^m, D_2^m))$	\mathcal{J}_{18}
	(F_{12}, F_{22}) and $\phi_2 > 0$	$(0, \min(r_1 m_1, D_1^*, D_1^m, D_2^m))$	\mathcal{J}_{19}
	$(\max(F_{12}, F_{22}), +\infty)$	$(0, \min(r_1 m_1, r_2 m_2, D_1^*, D_1^m, D_2^m))$	\mathcal{J}_{20}
$(S_2^m, +\infty)$	$[0, \lambda_1^2]$	$(D_2^m, +\infty)$	\mathcal{J}_0
	$\lambda_1^2, +\infty)$	$(D_2^m, +\infty)$	\mathcal{J}_1
	$\lambda_1^2, +\infty)$	(D_2^*, D_2^m)	\mathcal{J}_2
	$[0, \lambda_1^2]$	(D_2^*, D_2^m)	\mathcal{J}_3
	$[0, \lambda_1^2]$	(D_1^m, D_2^*)	\mathcal{J}_4
	$(\lambda_1^2, \min(\lambda_1^1, F_{22}))$	$(D_1^m, r_1 m_1)$	\mathcal{J}_5
	$(F_{22}, +\infty)$	$(D_1^*, \min(r_2 m_1, D_1^m, D_2^m))$	\mathcal{J}_{10}
	(λ_1^1, F_{22}) and $\phi_2 > 0$	$(D_1^*, \min(r_1 m_1, D_1^m, D_2^m))$	\mathcal{J}_{11}
	(λ_1^1, F_{22}) and $\phi_2 < 0$	$(D_1^*, \min(r_1 m_1, D_1^m, D_2^m))$	\mathcal{J}_{12}
	$(\lambda_1^2, \max(\lambda_1^1, F_{22}))$	$(D_1^*, \min(r_2 m_1, D_1^m))$	\mathcal{J}_{13}
	$[0, \lambda_1^2]$	(D_1^*, D_1^m)	\mathcal{J}_{14}
	$(\max(\lambda_1^1, \lambda_1^2), \min(F_{12}, F_{22}))$ and $\phi_2 > 0$	$(0, \min(r_1 m_1, r_2 m_1, D_2^m))$	\mathcal{J}_{21}
	$(\max(\lambda_1^1, F_{22}), F_{12})$	$(0, \min(r_1 m_1, r_2 m_1, D_2^m))$	\mathcal{J}_{22}
	(F_{22}, λ_1^1)	$(0, \min(r_2 m_1, D_1^*, D_2^m))$	\mathcal{J}_{23}
	$(F_{22}, +\infty)$	$(D_1^*, \min(r_2 m_1, D_1^m, D_2^m))$	\mathcal{J}_{24}
$[0, S_2^m)$	$[0, \lambda_1^2]$	$(D_2^*, +\infty)$	\mathcal{J}_0
	$(\lambda_1^2, F_{21}) \cup [\lambda_1^2, +\infty)$	$(D_2^m, +\infty) \cup (D_2^*, +\infty)$	\mathcal{J}_1
	(F_{21}, F_{22})	$(D_2^*, \min(r_2 m_1, D_2^m))$	\mathcal{J}_{25}
	$(F_{22}, +\infty)$	$(D_2^*, \min(r_2 m_1, D_2^m))$	\mathcal{J}_{26}
	$(F_{22}, +\infty)$	$(D_1^*, \min(r_2 m_1, D_1^m, D_2^m))$	\mathcal{J}_{27}
	(F_{12}, F_{22}) and $\phi_2 > 0$	$(D_1^*, \min(r_1 m_1, D_1^m))$	\mathcal{J}_{28}
	(F_{12}, F_{22}) and $\phi_2 < 0$	$(D_1^*, \min(r_1 m_1, D_1^m))$	\mathcal{J}_{29}
	(F_{11}, F_{12})	$(D_1^*, \min(r_1 m_1, D_1^m))$	\mathcal{J}_{30}
	(λ_1^1, F_{11})	$(D_1^*, \min(r_1 m_1, D_1^m))$	\mathcal{J}_{31}
	$(\lambda_1^2, \min(\lambda_1^1, F_{22}))$	$(D_1^*, \min(r_2 m_1, D_2^*))$	\mathcal{J}_5
	$[0, \lambda_1^2]$	(D_1^*, D_2^*)	\mathcal{J}_4

- [18] A. Donoso-Bravo, P. Gajardo, M. Sebbah and D. Vicencio, Comparison of performance in an anaerobic digestion process: one-reactor vs two-reactor configurations, *Math. Biosci. Eng.*, **16**, 2447–2465 (2019).
- [19] R. Fekih-Salem, Y. Daoud, N. Abdellatifi and T. Sari, A mathematical model of anaerobic digestion with syntrophic relationship, substrate inhibition and distinct removal rates, *SIAM J. Appl. Dyn. Syst. (SIADS)*, **20**, 1621–1654 (2021).
- [20] R. Fekih-Salem, C. Lobry and T. Sari, A density-dependent model of competition for one resource in the chemostat, *Math. Biosci.*, **286**, 104–122 (2017).
- [21] C.D.D. Gooijer, W.A.M. Bakker, H.H. Beertink and J. Tramper, Bioreactors in series: An overview of design procedures and practical applications, *Enzyme Microb. Technol.*, **18**, 202–219 (1996).
- [22] I. Haidar, A. Rapaport, F. Gérard, Effects of spatial structure and diffusion on the performances of the chemostat, *Math. Biosci. Eng.*, **8**, 953–971 (2011).
- [23] M. Hanaki, J. Harmand, Z. Mghazli, A. Rapaport, T. Sari and P. Ugalde, Mathematical study of a two-stage anaerobic model when the hydrolysis is the limiting step, *Processes*, **9**, 2050 (2021).
- [24] J. Harmand, C. Lobry, A. Rapaport, and T. Sari, *The Chemostat: Mathematical Theory of Microorganism*

Table 14

Definitions of the regions \mathcal{J}_i , $i = 0, 20-22, 32-46$ of the operating diagram of Figure 5 in the case $r \in (1/2, 1)$ and $S_2^{in} \in (S_2^m, +\infty)$. The functions D_i^m and D_i^* , $i = 1, 2$ are defined in Table 6 while the functions F_{ij} and ϕ_2 , $i, j = 1, 2$ are defined in Table 1.

S_1^{in} and ϕ_2	Condition on D	Region
$[0, \lambda_1^1)$	$(D_1^m, +\infty)$	\mathcal{J}_0
$\left. \begin{array}{l} [\lambda_1^1, +\infty) \\ [\lambda_1^1, +\infty) \end{array} \right\}$	$(D_1^m, r_1 m_1)$	\mathcal{J}_{32}
$\left. \begin{array}{l} [\lambda_1^1, +\infty) \\ [0, \lambda_1^1) \end{array} \right\}$	$(D_1^*, \min(r_1 m_1, D_1^m))$	\mathcal{J}_{33}
$[0, \lambda_1^1)$	(D_1^*, D_1^m)	\mathcal{J}_{34}
$[0, \lambda_1^1)$	(D_2^m, D_1^*)	\mathcal{J}_{35}
$(\lambda_1^1, \min(\lambda_1^2, F_{12}))$	$(D_2^m, r_1 m_1)$	\mathcal{J}_{36}
(λ_1^2, F_{12})	$(D_2^m, r_2 m_1)$	\mathcal{J}_{37}
(F_{12}, λ_1^2)	$[0, \min(r_1 m_1, D_1^*, D_1^m))$	\mathcal{J}_{38}
$(\max(\lambda_1^2, F_{12}), +\infty)$	$(D_2^m, \min(r_1 m_1, r_2 m_1, D_1^m))$	\mathcal{J}_{39}
$(F_{12}, +\infty)$	$(D_2^*, \min(r_1 m_1, D_1^*, D_2^m))$	\mathcal{J}_{40}
(λ_1^2, F_{12})	$(D_2^*, \min(r_2 m_1, D_2^m))$	\mathcal{J}_{41}
$(\lambda_1^1, \lambda_1^2)$	$(D_2^*, \min(r_1 m_1, D_2^m))$	\mathcal{J}_{42}
$[0, \lambda_1^1)$	(D_2^*, D_2^m)	\mathcal{J}_{43}
$[0, \lambda_1^1)$	$(0, D_2^*)$	\mathcal{J}_{15}
$(\lambda_1^1, \lambda_1^2)$ and $\phi_2 < 0$	$(0, \min(r_1 m_1, D_2^*, D_2^m))$	\mathcal{J}_{44}
$(\lambda_1^1, \lambda_1^2)$ and $\phi_2 > 0$	$(0, \min(r_1 m_1, D_2^*, D_2^m))$	\mathcal{J}_{45}
(λ_1^2, F_{22}) and $\phi_2 < 0$	$(0, \min(r_1 m_1, r_2 m_1, D_2^m))$	\mathcal{J}_{46}
(λ_1^2, F_{22}) and $\phi_2 > 0$	$(0, \min(r_1 m_1, r_2 m_1, D_2^m))$	\mathcal{J}_{21}
(F_{22}, F_{12})	$(0, \min(r_2 m_1, D_2^*, D_2^m))$	\mathcal{J}_{22}
$(F_{12}, +\infty)$	$(0, \min(r_1 m_1, D_2^*, D_1^m))$	\mathcal{J}_{20}

Cultures, Chemical Eng. Ser., ISTE-Wiley, New York (2017).

- [25] J. Harmand, A. Rapaport and D. Dochain, Increasing the dilution rate can globally stabilize two-step biological systems, *J. Proc. Control*, **95**, 67–74 (2020).
- [26] J. Harmand, A. Rapaport and A. Dramé, Optimal design of two interconnected enzymatic reactors, *J. Proc. Control*, **14**, 785–794 (2004).
- [27] J. Harmand, A. Rapaport and A. Trofino, Optimal design of two interconnected bioreactors some new results, *AIChE J.*, **49** (2003), 1433–1450.
- [28] A. Isidori, *Nonlinear Control Systems II*, Springer-Verlag, London (1999).
- [29] IWA Publishing, IWA task group for mathematical modelling of anaerobic digestion processes, Anaerobic Digestion Model No.1 (ADM1). Scientific and Technical Report No. 13, IWA Publishing, London (2002).
- [30] Z. Khedim, B. Benyahia, B. Cherki, T. Sari and J. Harmand, Effect of control parameters on biogas production during the anaerobic digestion of protein-rich substrates, *Appl. Math. Model.*, **61**, 351–376 (2018).
- [31] O. Levenspiel, *Chemical reaction engineering*, 3rd Edition, Wiley, New York, New York (1998).
- [32] J. Monod, The technique of a continuous culture. Theory and applications, *Ann. Inst. Pasteur*, **79**, 390–410 (1950).
- [33] T. Mtar, R. Fekih-Salem and T. Sari, Interspecific density-dependent model of predator-prey relationship in the chemostat, *Int. J. Biomath.*, **14**, 2050086 (2021).
- [34] T. Mtar, R. Fekih-Salem and T. Sari, Mortality can produce limit cycles in density-dependent models with a predator-prey relationship, *Discrete and Continuous Dyn. Syst. - B*, **27**, 7445–7467 (2022).
- [35] S. Nouaoura, N. Abdellatif, R. Fekih-Salem and T. Sari, Mathematical analysis of a three-tiered model of anaerobic digestion, *SIAM J. Appl. Math.*, **81**, 1264–1286 (2021).
- [36] S. Nouaoura, R. Fekih-Salem, N. Abdellatif and T. Sari, Mathematical analysis of a three-tiered food-web in the chemostat, *Discrete and Continuous Dyn. Syst. - B*, **26**, 5601–5625 (2021).
- [37] S. Nouaoura, R. Fekih-Salem, N. Abdellatif, T. Sari, Operating diagrams for a three-tiered microbial food web in the chemostat, *J. Math. Biol.*, **85**, 7445–7467 (2022).
- [38] A. Novick and L. Szilard, Description of the chemostat, *Science*, **112**, 715–716 (1950).
- [39] N. Pan, H. Wang, Y. Tian, E. Chorukova, I. Simeonov and N. Christov, Comparison Study of Dynamic Models for One-stage and Two-stage Anaerobic Digestion Processes, *IFAC-PapersOnLine*, **55**, 667–672

Table 15

Definitions of the regions \mathcal{J}_i , $i = 0, 1, 4, 5, 15, 27, 46 - 69$ of the operating diagram of Figure 6 in the plane (S_2^{in}, S_1^{in}) when $r \in (0, 1/2)$ and $D \in (0, \mu_2(S_2^m))$. For $i, j = 1, 2$, the functions D_i^m and D_i^* are defined in Table 6 while the functions F_{ij} and ϕ_2 in Table 1.

Condition on		
S_2^{in}	S_1^{in} and ϕ_2	Region
$[0, \lambda_2^{21})$	$[0, \lambda_1^2)$	\mathcal{J}_0
	(λ_1^2, F_{21})	\mathcal{J}_1
	(F_{21}, λ_1^1)	\mathcal{J}_{64}
	(λ_1^1, F_{11})	\mathcal{J}_{65}
	(F_{11}, F_{12})	\mathcal{J}_{66}
	(F_{12}, F_{22}) and $\phi_2 < 0$	\mathcal{J}_{67}
	(F_{12}, F_{22}) and $\phi_2 > 0$	\mathcal{J}_{68}
	$(F_{22}, +\infty)$	\mathcal{J}_{69}
$(\lambda_2^{21}, \lambda_2^{11})$	$[0, \lambda_1^2)$	\mathcal{J}_4
	$(\lambda_1^2, \lambda_1^1)$	\mathcal{J}_5
	(λ_1^1, F_{11})	\mathcal{J}_{63}
	(F_{11}, F_{12})	\mathcal{J}_{62}
	(F_{12}, F_{22}) and $\phi_2 < 0$	\mathcal{J}_{61}
	(F_{12}, F_{22}) and $\phi_2 > 0$	\mathcal{J}_{60}
	$(F_{22}, +\infty)$	\mathcal{J}_{27}
$(\lambda_2^{11}, \lambda_2^{12})$	$[0, \lambda_1^2)$	\mathcal{J}_{15}
	$(\lambda_1^2, \lambda_1^1)$	\mathcal{J}_{56}
	(λ_1^1, F_{12})	\mathcal{J}_{46}
	(F_{12}, F_{22}) and $\phi_2 < 0$	\mathcal{J}_{57}
	(F_{12}, F_{22}) and $\phi_2 > 0$	\mathcal{J}_{58}
	$(F_{22}, +\infty)$	\mathcal{J}_{59}
$(\lambda_2^{12}, \lambda_2^{22})$	$(\max(\lambda_1^1, F_{22}), +\infty)$	\mathcal{J}_{50}
	(λ_1^1, F_{22}) and $\phi_2 > 0$	\mathcal{J}_{51}
	(λ_1^1, F_{22}) and $\phi_2 < 0$	\mathcal{J}_{52}
	(F_{22}, λ_1^1)	\mathcal{J}_{53}
	$(\lambda_1^2, \min(\lambda_1^1, F_{22}))$	\mathcal{J}_{54}
	$[0, \lambda_1^2)$	\mathcal{J}_{55}
$(\lambda_2^{22}, +\infty)$	$[0, \lambda_1^2)$	\mathcal{J}_{47}
	$(\lambda_1^2, \lambda_1^1)$	\mathcal{J}_{48}
	$(\lambda_1^1, +\infty)$	\mathcal{J}_{49}

(2022).

- [40] T. Sari, Best operating conditions for biogas production in some simple anaerobic digestion models, *Processes*, **10**, 258 (2022).
- [41] T. Sari and B. Benyahia, The operating diagram for a two-step anaerobic digestion model, *Nonlinear Dyn.*, **105**, 2711–2737 (2021).
- [42] T. Sari and J. Harmand, A model of a syntrophic relationship between two microbial species in a chemostat including maintenance, *Math. Biosci.*, **275**, 1–9 (2016).
- [43] T. Sari and M.J. Wade, Generalised approach to modelling a three-tiered microbial food-web, *Math. Biosci.*, **291**, 21–37 (2017).
- [44] M. Sbarciog, M. Loccufier and E. Noldus, Determination of appropriate operating strategies for anaerobic digestion systems, *Biochem. Eng. J.*, **51**, 180–188 (2010).
- [45] A. Schievano, A. Tenca, S. Lonati, E. Manzini and F. Adani, Can two-stage instead of one-stage anaerobic digestion really increase energy recovery from biomass?, *Appl. Energy*, **124**, 335–342 (2014).
- [46] H. L. Smith and P. Waltman, *The Theory of the Chemostat: Dynamics of Microbial Competition*, Cambridge University Press, Cambridge, UK (1995).
- [47] S. Sobieszek, M.J. Wade and G.S.K. Wolkowicz, Rich dynamics of a three-tiered anaerobic food-web in a chemostat with multiple substrate inflow, *Math. Biosci. Eng.*, **17**, 7045–7073 (2020).
- [48] P.M.V. Subbarao, T.C. D'Silva, K. Adlak, S. Kumar, R. Chandra and V. K. Vijay, Anaerobic digestion as

- a sustainable technology for efficiently utilizing biomass in the context of carbon neutrality and circular economy, *Environ. Res.*, **234**, 116286 (2023).
- [49] M. J. Wade, J. Oakley, S. Harbisher, N. G. Parker and J. Doling, MI-Sim: A MATLAB package for the numerical analysis of microbial ecological interactions, *PLoS ONE.*, **12**, e0173249 (2017).
 - [50] M.J. Wade, R.W. Pattinson, N.G. Parker and J. Doling, Emergent behaviour in a chlorophenol-mineralising three-tiered microbial ‘food web’, *J. Theor. Biol.*, **389**, 171–186 (2016).
 - [51] M. Weedermaun, G. Seo and G.S.K. Wolkowicz, Mathematical model of anaerobic digestion in a chemostat: effects of syntrophy and inhibition, *J. Biol. Dyn.*, **7**, 59–85 (2013).
 - [52] M. Weedermaun, G.S.K. Wolkowicz and J. Sasarag, Optimal biogas production in a model for anaerobic digestion, *Nonlinear Dyn.*, **81**, 1097–1112 (2015).
 - [53] A. Xu, J. Doling, T.P. Curtis, G. Montague, E. Martin, Maintenance affects the stability of a two-tiered microbial ‘food chain’?, *J. Theor. Biol.*, **276**, 35–41 (2011).
 - [54] N.E.H. Zitouni, M. Dellal and M. Lakrib, Substrate inhibition can produce coexistence and limit cycles in the chemostat model with allelopathy, *J. Math. Biol.*, **87:7**, 35–41 (2023).